

Twins & Dislocations in HCP Textbook & Paper Reviews

Cindy Smith

Outline

- Motivation
- Review:
 - Crystal lattices (fcc, bcc, hcp)
 - Fcc vs. hcp stacking sequences
 - Cubic $\{hkl\}$ naming
 - Hcp $\{hkil\}$ naming
 - Twinning theory
 - TEM images of twins
- Hcp twins & dislocations schematics and notation
- Hcp twin & dislocation interaction computer modeling done by A. Serra, D.J. Bacon, & R.C. Pond (next week)

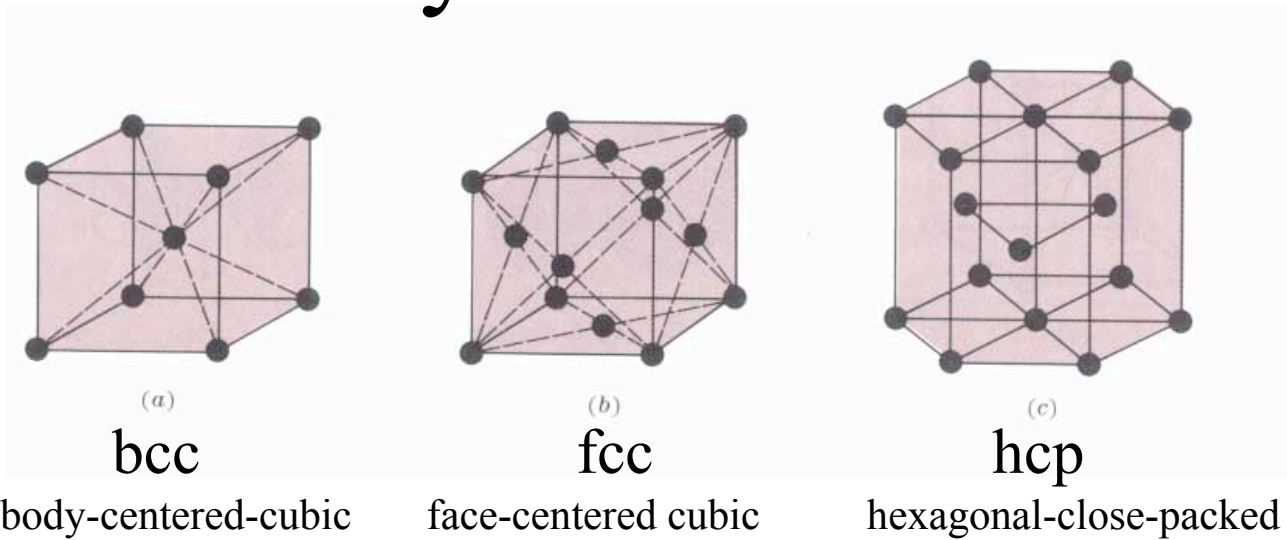
Motivation

- The mechanical response of hexagonal close-packed (hcp) metals is strongly dependent on the combination of active deformation modes, both slip and twinning.
 - This is in turn dependent on the c/a ratio, available deformation modes, critical resolved shear stress (CRSS) for slip, and twin activation stress.
- Deformation-induced twins may act as barriers to further slip
 - Some twin-dislocation interactions can actually assist twin boundary motion under stress.
- Dislocation movement into or along a twin boundary depends on the atomic arrangement at the interface and the dislocation core
 - Serra, *et.al.*, used atomistic computer simulation to investigate this, instead of the classic purely crystallographic explanation or the continuum description.

Motivation

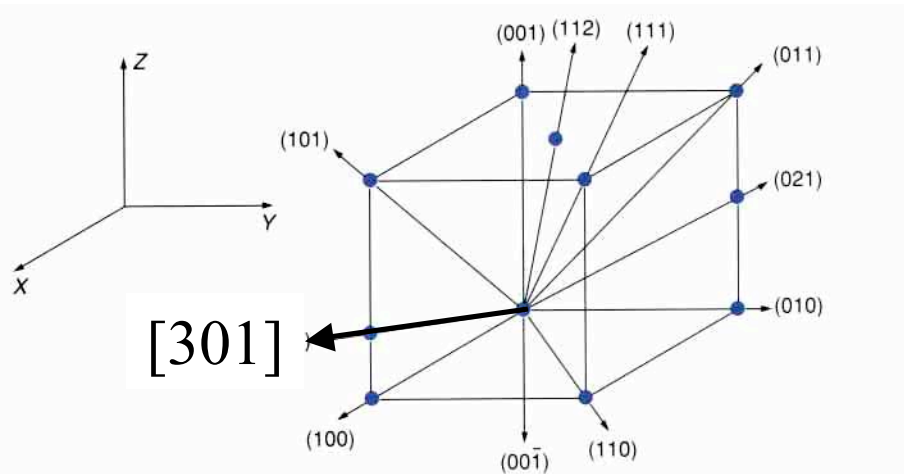
- Zirconium is a good representative hcp metal because it is readily deformable, and exhibits a manageable number of slip and twinning systems.
- For typical hcp metals, the primary systems are:
 - Basal slip $\{0001\}\langle\bar{1}\bar{2}10\rangle$
 - Prismatic slip $\{10\bar{1}0\}\langle\bar{1}\bar{2}10\rangle$
 - Pyramidal twins $\{10\bar{1}1\}$
- At room temperature and below for Zr, the systems are:
 - Prismatic slip $\{10\bar{1}0\}\langle\bar{1}\bar{2}10\rangle$
 - Tension twins $\{10\bar{1}2\}\langle\bar{1}011\rangle$, and $\{11\bar{2}1\}\langle\bar{1}\bar{1}26\rangle$
 - Compression twin $\{11\bar{2}2\}\langle\bar{1}\bar{1}23\rangle$
 - And secondary pyramidal slip may play a limited role at RT $\{10\bar{1}1\}\langle\bar{2}113\rangle$, or $\{11\bar{2}1\}\langle\bar{2}113\rangle$

Crystal lattices



Various views of hcp lattice

Cubic Miller Indices



Miller indices of directions in cubic lattices. After C. R. Barrett, W. D. Nix and A. S. Tetelman, *The Principles of Engineering Materials*, Prentice-Hall, Englewood Cliffs, NJ (1973).

Vectors from one point to another are reduced to the smallest whole numbers, i.e. $[1\ 0\ 1/3]$ becomes $[301]$

Any three points define a plane:

- 1) Express the intercepts of the plane on the three coordinate axes in number of unit cell dimensions.
- 2) Take reciprocals of these numbers.
- 3) Reduce reciprocals to smallest integers by clearing fractions.

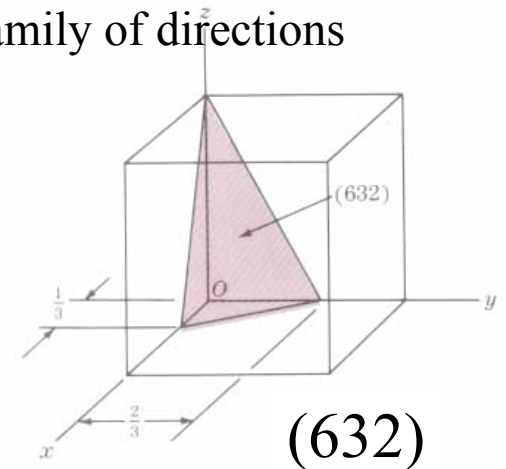
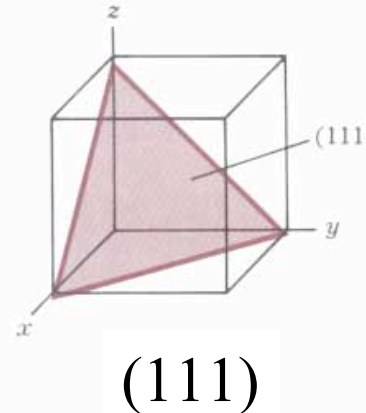
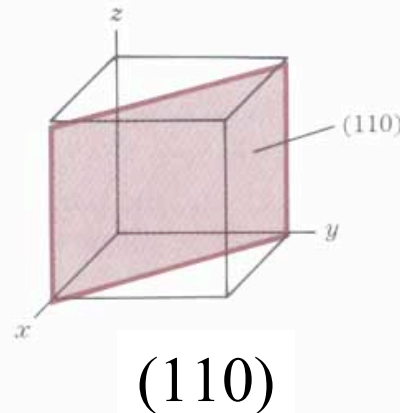
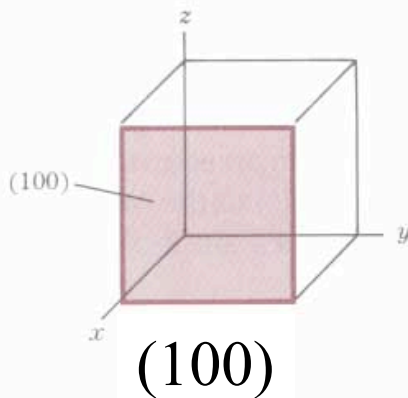
Note that the (hkl) planes are perpendicular to the $[hkl]$ vectors.

(hkl) = a plane

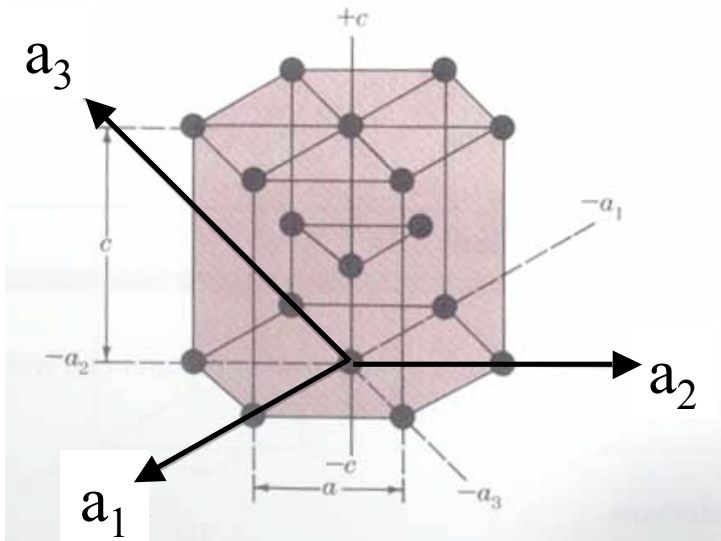
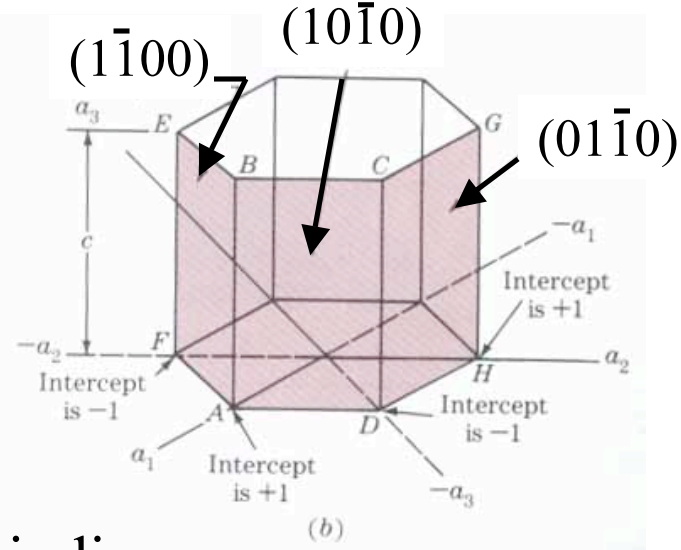
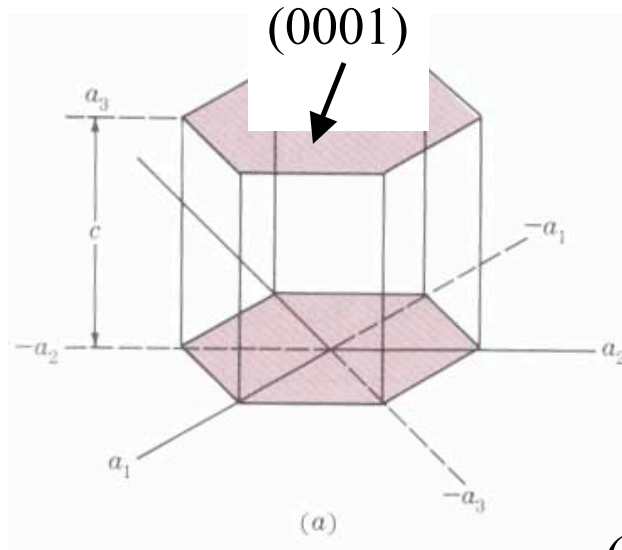
$\{hkl\}$ = a family of planes

$[uvw]$ = a direction (vector)

$\langle uvw \rangle$ = a family of directions



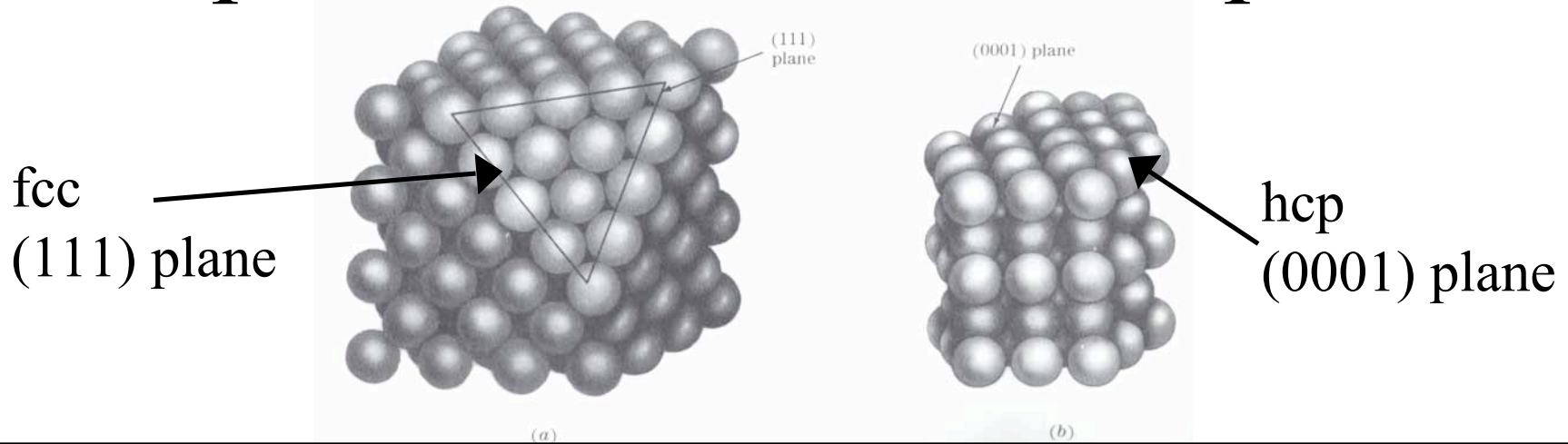
HCP crystal Miller-Bravais indices



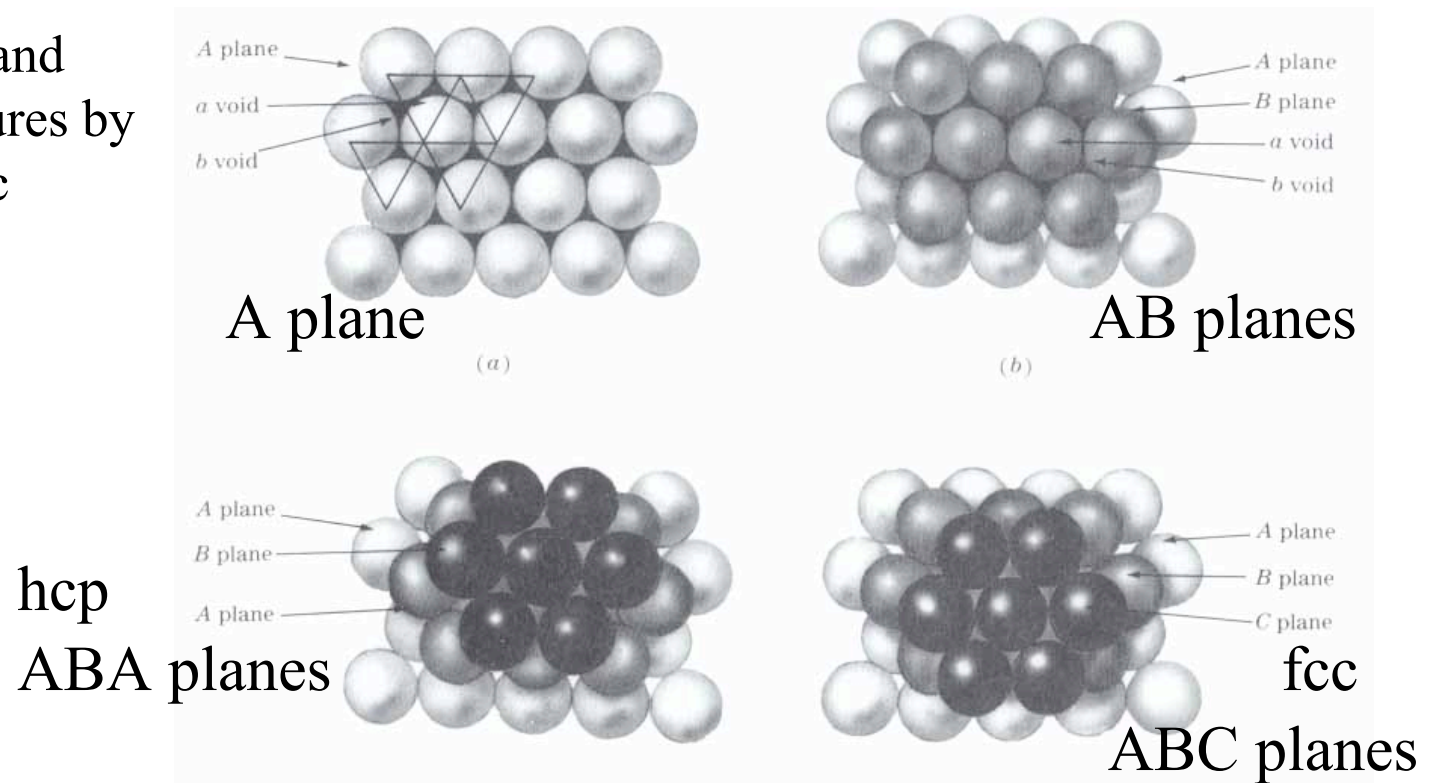
(hkil) indices:

- Three basal axes, a_1 , a_2 , a_3 , which are 120 degrees to each other. (The h, k, and i indices.)
- Fourth axis, c, is vertical along the unit cell (the l index).
- HCP planes are sometimes identified by only three indices (hkl) as $h + k = -i$
- Directions can similarly be indicated by four indices as $[uvtw]$, and $u + v = -t$

Hcp vs. fcc closed packed planes



Formation of fcc and hcp crystal structures by stacking of atomic planes



Hcp vs. fcc closed packed planes

ABC
stacking

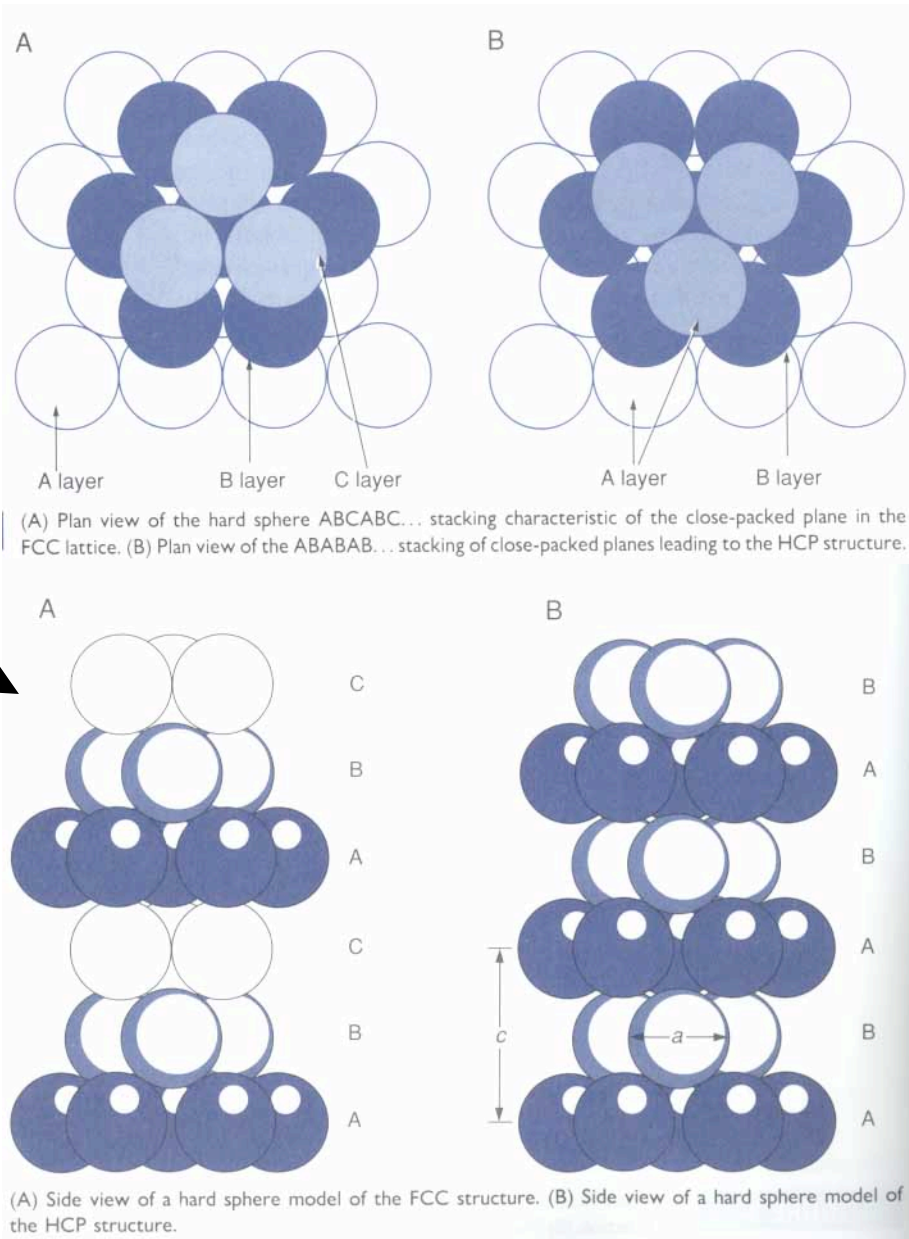
ABA
stacking

fcc

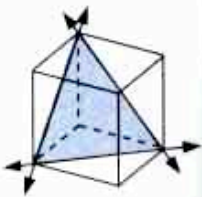
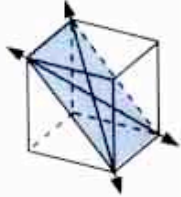
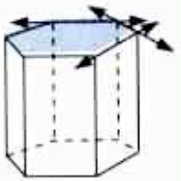
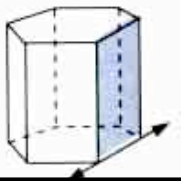
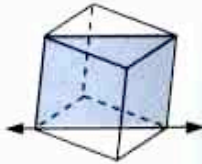
hcp

ABC
stacking

ABA
stacking



Dislocation Slip Systems

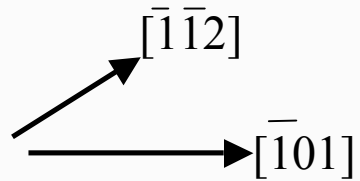
Structure and material	Slip plane	Slip direction	Number of slip systems	τ_{CRSS} (MPa)	Slip geometry
FCC Ag (99.99%) Cu (99.999%) Ni (99.8%)	{111}	$\langle \bar{1}10 \rangle$	$\{4\} \times \langle 3 \rangle = 12$	0.58 0.65 5.7	
Diamond cubic Si, Ge	{111}	$\langle \bar{1}10 \rangle$	$\{4\} \times \langle 3 \rangle = 12$		
BCC Fe (99.96%) Mo	{110} {110}	$\langle \bar{1}\bar{1}1 \rangle$ $\langle \bar{1}\bar{1}1 \rangle$	$\{6\} \times \langle 2 \rangle = 12$	27.5 49.0	
HCP Zn (99.999%) Cd (99.996%) Mg (99.996%) Al ₂ O ₃ , BeO Ti (99.99%)	(0001) (0001) (0001) (0001) (1010)	$[11\bar{2}0]$ $[11\bar{2}0]$ $[11\bar{2}0]$ $[11\bar{2}0]$ $[11\bar{2}0]$	$\{1\} \times \langle 3 \rangle = 3$ $\{1\} \times \langle 3 \rangle = 3$	0.18 0.58 0.77 13.7	 
Rocksalt LiF, MgO	(110)	$[1\bar{1}0]$	$\{6\} \times \langle 1 \rangle = 6$		

HCP primary slip system:
 $(0001)[11\bar{2}0]$

After H. W. Hayden, W. G. Moffatt, and J. Wulff, *The Structure and Properties of Materials*, Vol. III, Wiley, New York (1965).

Burgers vectors on close-packed planes

FCC perfect Burgers vector splits into two partials by the following equation:

$$\frac{a}{2}[\bar{1}01] = \frac{a}{6}[\bar{2}11] + \frac{a}{6}[\bar{1}\bar{1}2]$$


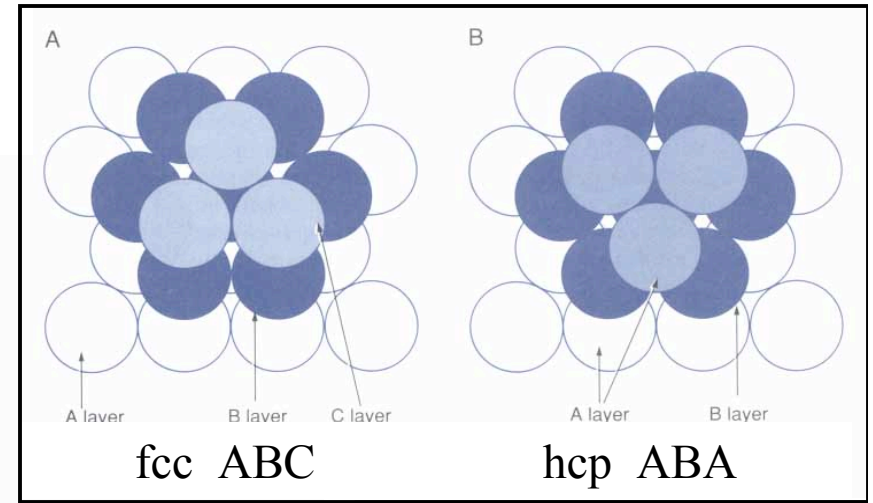
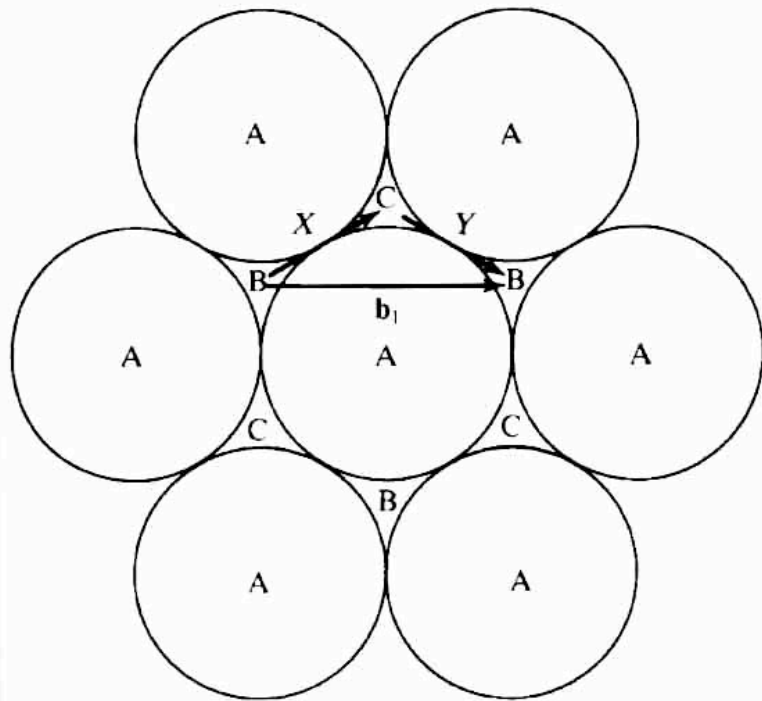
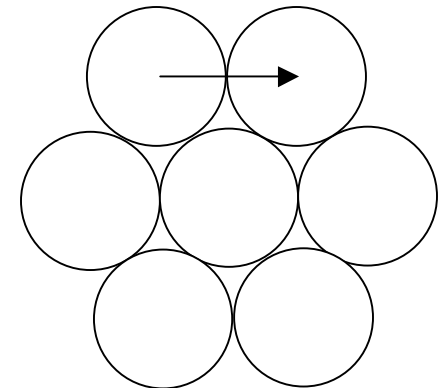


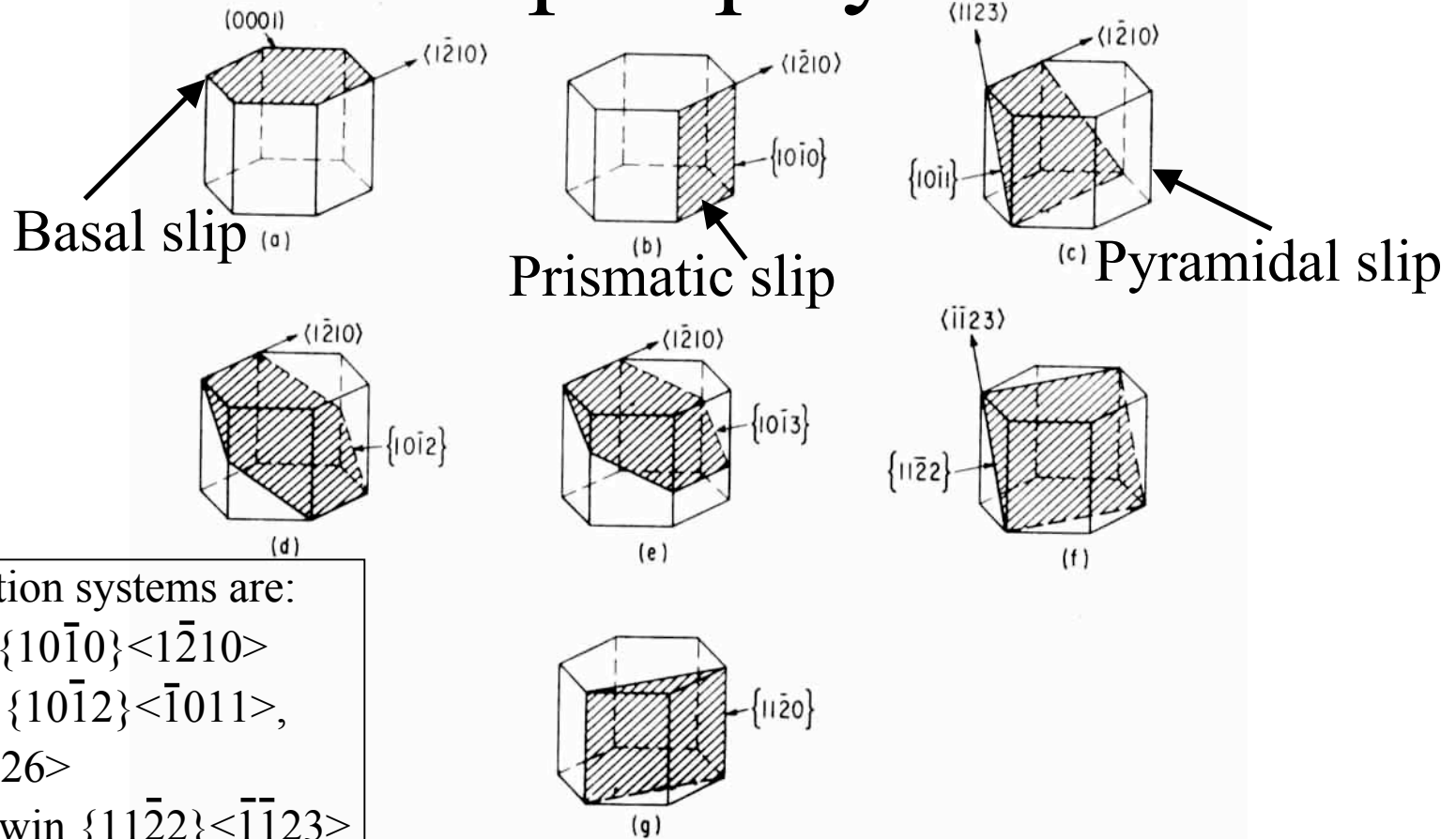
Figure 3.29

A portion of the atoms in a (111) plane in a fcc crystal. Unit slip in the B plane occurs with displacement $(a/2)[\bar{1}01]$. Instead of slip occurring by unit displacement it can take place in two segmental steps (X and Y). The displacement X results in atoms in plane B temporarily occupying a C stacking sequence in the fcc lattice.

Hcp basal slip
 $\langle \bar{1}210 \rangle$



Possible hcp slip systems



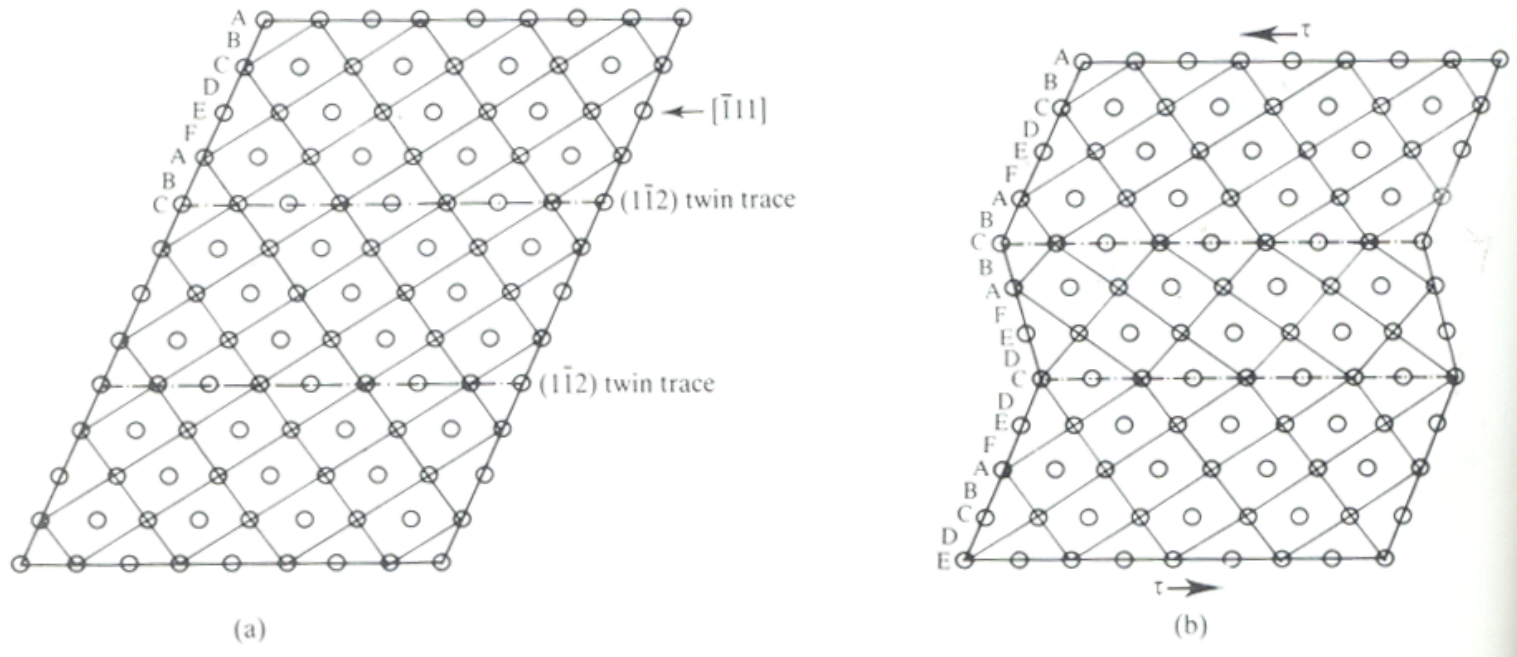
Zr RT deformation systems are:

- Prismatic slip $\{10\bar{1}0\}\langle 1\bar{2}10 \rangle$
- Tension twins $\{10\bar{1}2\}\langle \bar{1}011 \rangle$,
and $\{11\bar{2}1\}\langle \bar{1}\bar{1}26 \rangle$
- Compression twin $\{11\bar{2}2\}\langle \bar{1}\bar{1}23 \rangle$

Fig. 1. The planes and directions that are considered as possible slip systems are schematically shown.

- (a) Basal slip on $(0001)\langle 1\bar{2}10 \rangle$
 (b) Prismatic slip on $\{10\bar{1}0\}\langle 1\bar{2}10 \rangle$
 (c) $\{10\bar{1}1\}\langle 1\bar{2}10 \rangle$ and $\{10\bar{1}1\}\langle \bar{1}\bar{1}23 \rangle$
 (d) $\{10\bar{1}2\}\langle 1\bar{2}10 \rangle$
 (e) $\{10\bar{1}3\}\langle 1\bar{1}\bar{1}0 \rangle$
 (f) $\{11\bar{2}2\}\langle \bar{1}\bar{1}23 \rangle$
 (g) $\{11\bar{2}0\}$

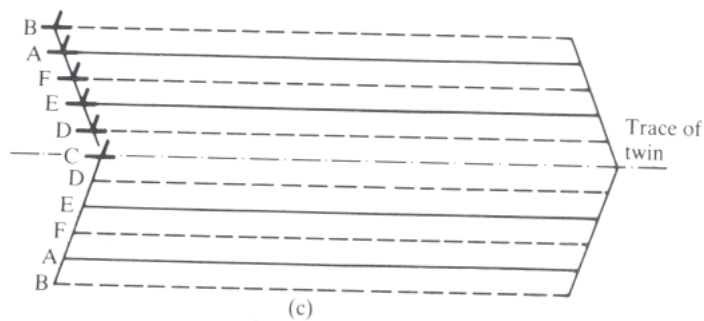
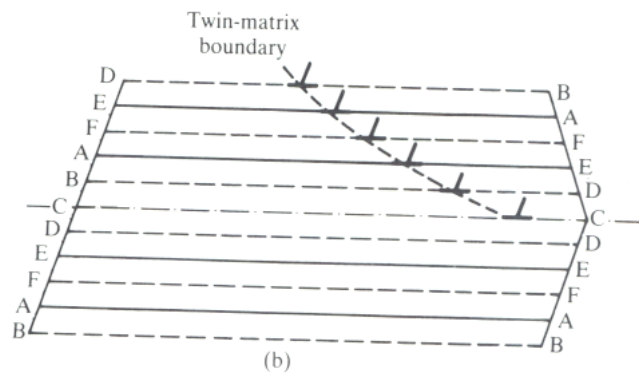
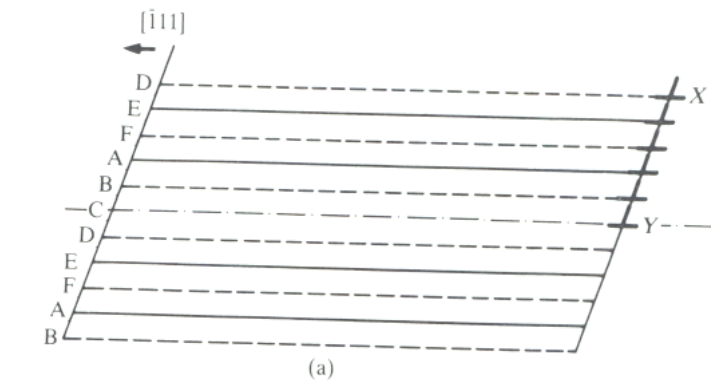
Twinning



Twinning deformation in the bcc crystal structure.

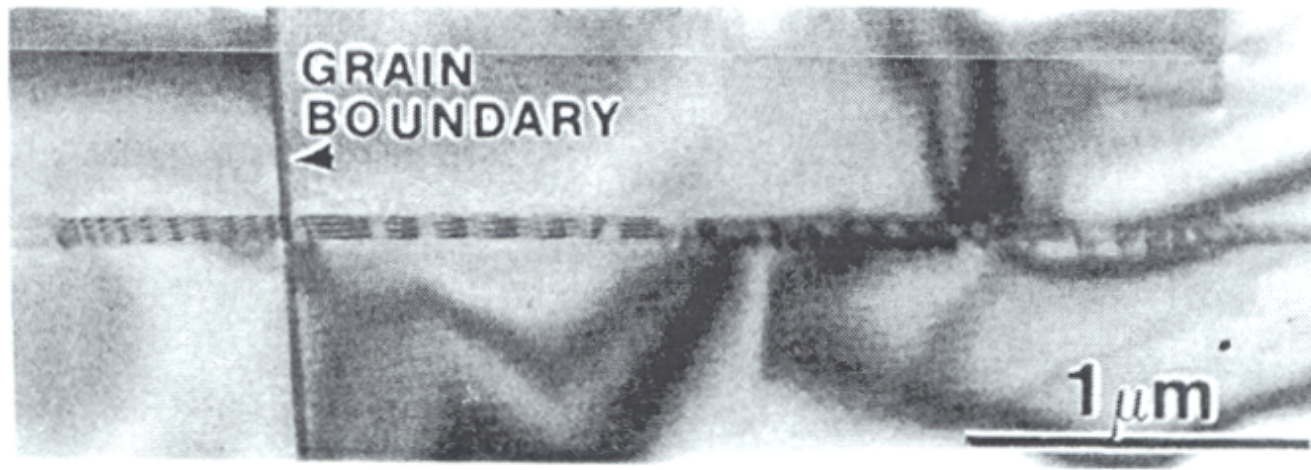
(a) The untwinned structure. (b) Twinning occurs by cooperative displacement of atoms in the $[\bar{1}\bar{1}1]$ direction. The result of twinning is to produce a permanent shape change (plastic deformation).

A Twinning mechanism



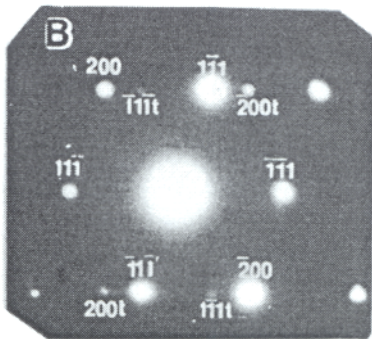
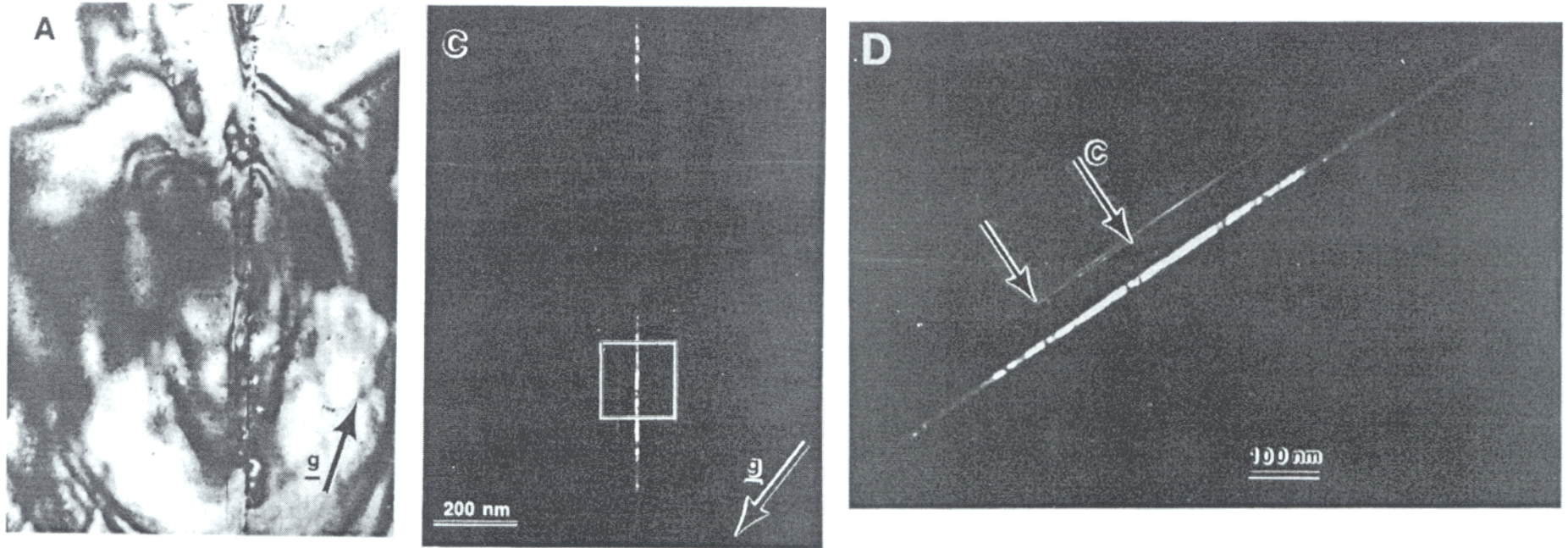
Mechanical twinning by edge-dislocation motion. In (a) the stacking in the unstressed crystal is schematized in a manner similar to the previous picture. (b) Motion of the dislocations in the $[11\bar{1}]$ direction produces the twin misorientation and in (c) the process is complete.

TEM image of microtwin



At some small angle boundaries, the twin fault can propagate across the boundary. Different fringe structures can be seen on either side of the boundary. Most likely the stress due to the pile-up of fault dislocations against one side of the g.b. nucleated and propagated a new fault in the adjacent grain.

TEM images of microtwins



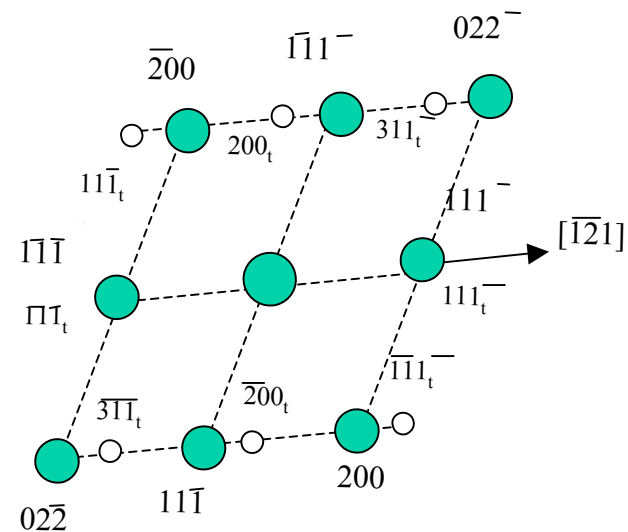
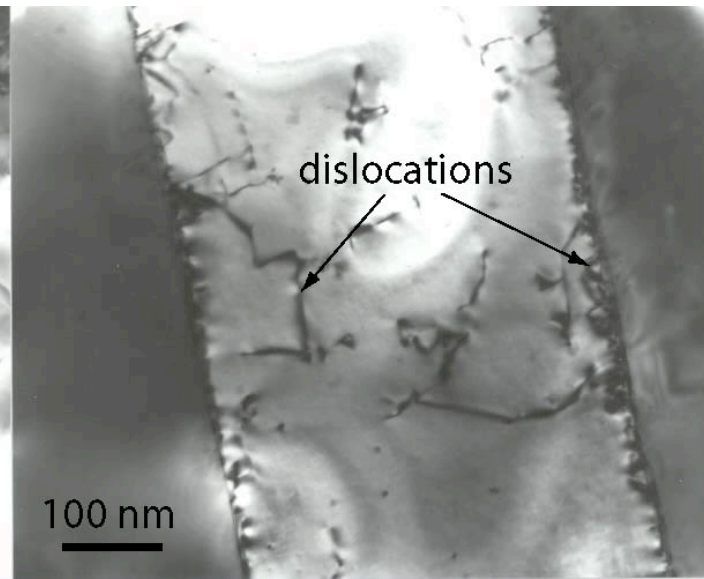
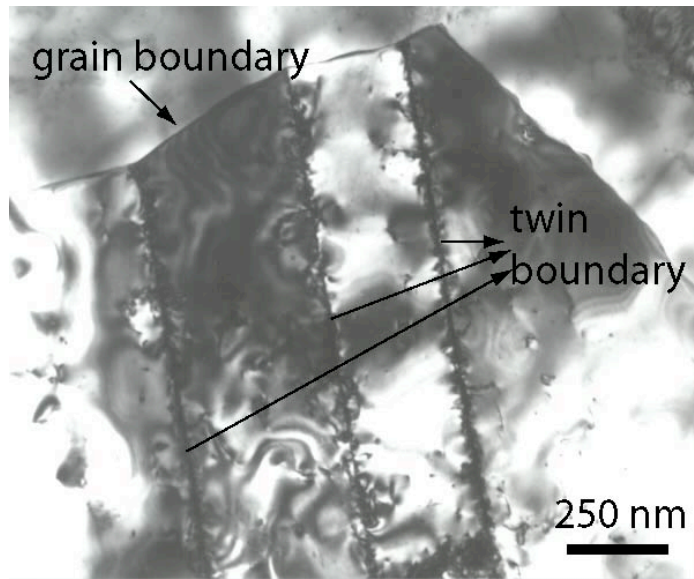
(A) BF of microtwin parallel to electron beam.

(B) Diffraction pattern showing twin spots

(C) DF using the (200) twin spot

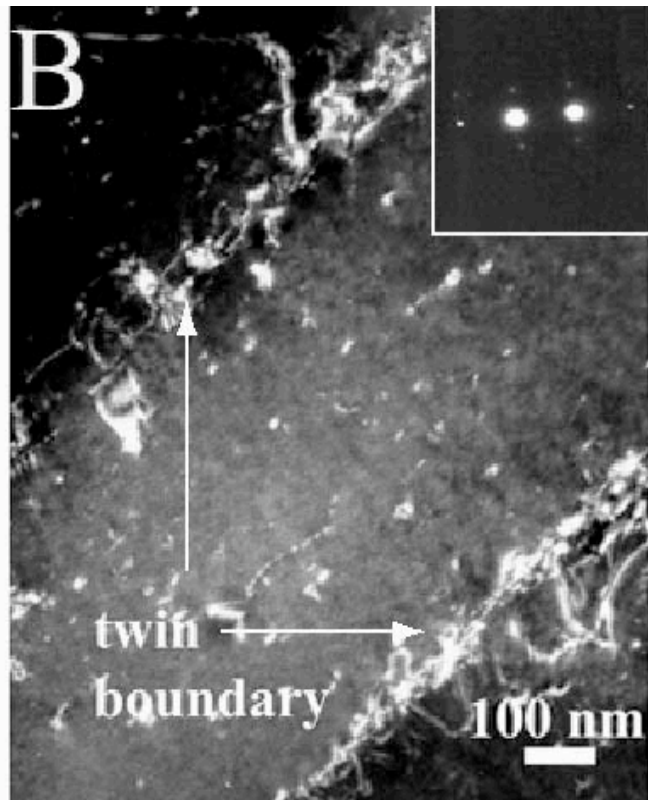
(D) Boxed area in C at higher magnification showing a thin twin parallel to the main twin.

TEM Examples of Twins

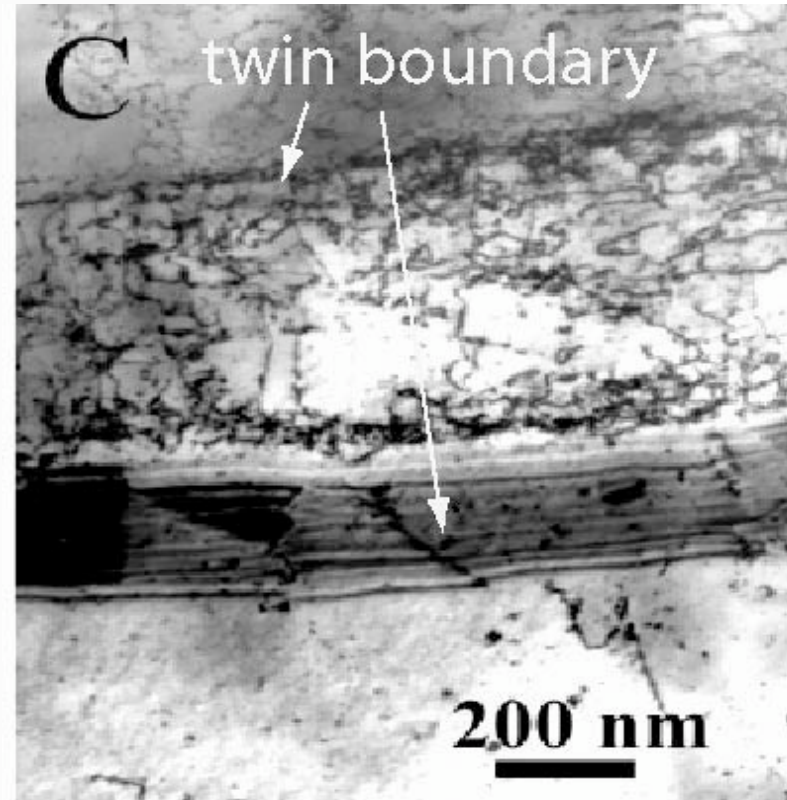


TEM Examples of Twins

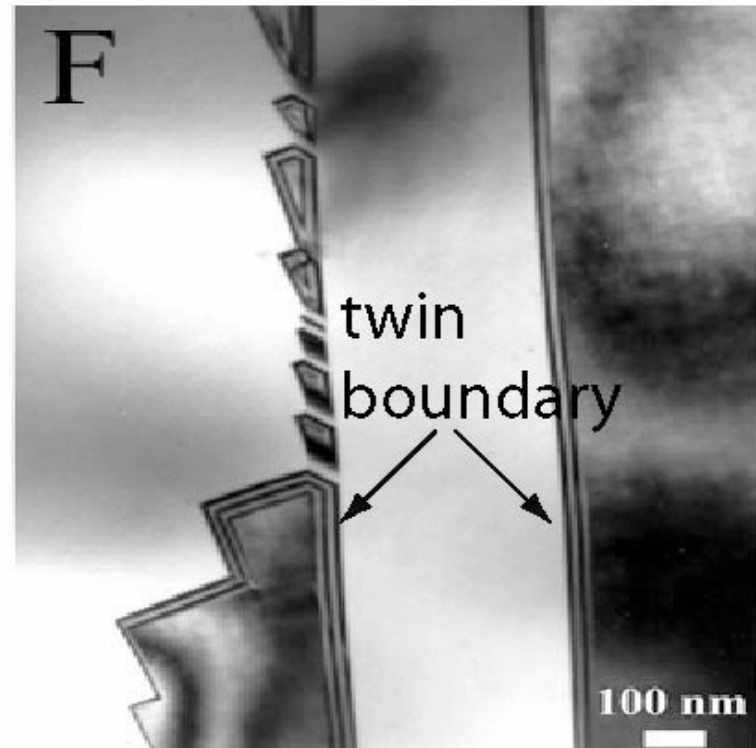
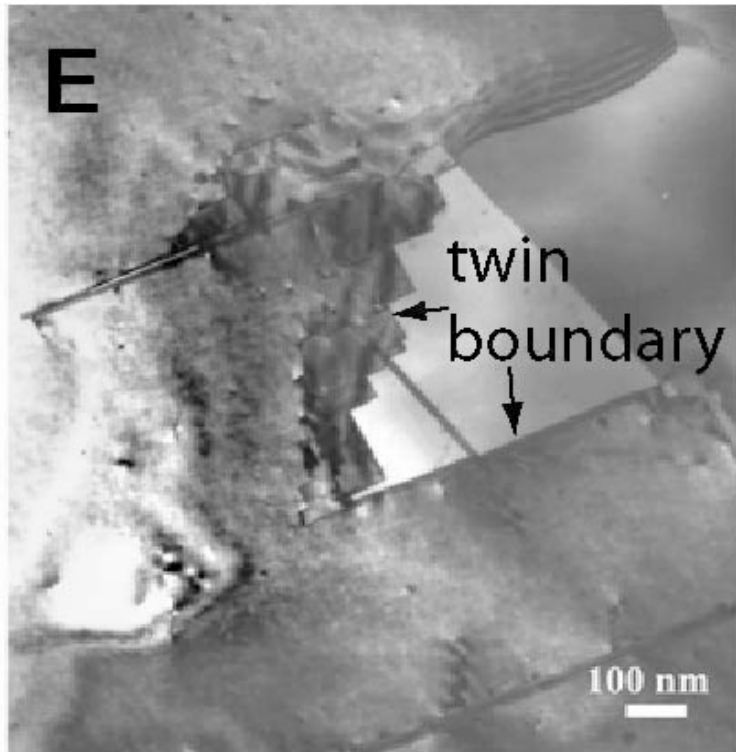
WBDF image



BF image



TEM Examples of Twins



Twins & Dislocations in HCP (continued)

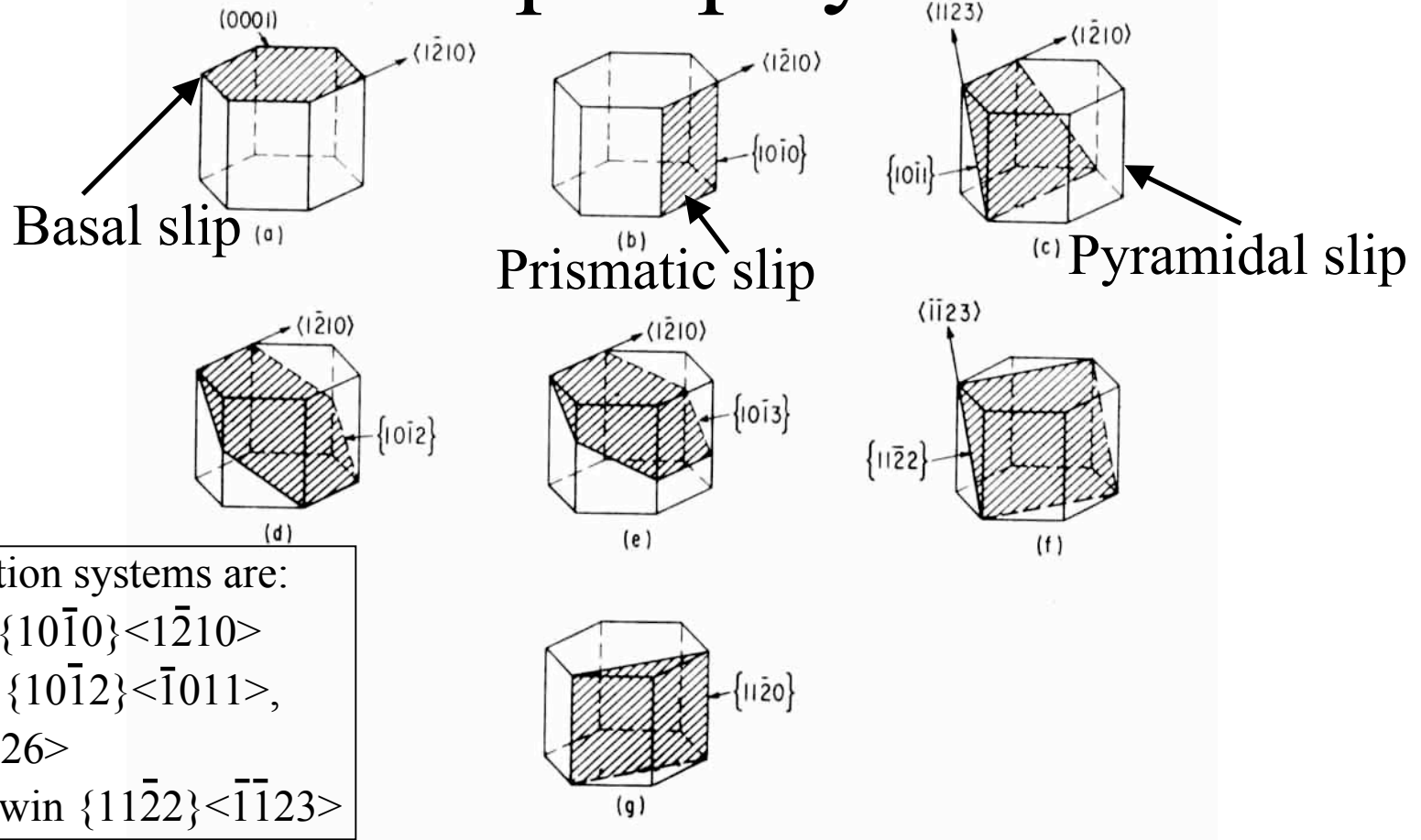
Cindy Smith

7/15/03

Outline

- Review of hcp slip systems
- Twinning as a function of temperature
- Twinning shear vs. c/a ratio
- Notation for twinning planes and directions (K_1 , K_2 , η_1 , η_2)
- Notation for schematics of twins
- Notation for dichromatic patterns
- Notation for interface burgers vectors
- The approach and model used by Serra, et.al.
- The Results of Serra, et.al.

Possible hcp slip systems



Zr RT deformation systems are:

- Prismatic slip $\{10\bar{1}0\}\langle 1\bar{2}10 \rangle$
- Tension twins $\{10\bar{1}2\}\langle \bar{1}011 \rangle$,
and $\{11\bar{2}1\}\langle \bar{1}\bar{1}26 \rangle$
- Compression twin $\{11\bar{2}2\}\langle \bar{1}\bar{1}23 \rangle$

Fig. 1. The planes and directions that are considered as possible slip systems are schematically shown.

- (a) Basal slip on $(0001)\langle 1\bar{2}10 \rangle$
 (b) Prismatic slip on $\{10\bar{1}0\}\langle 1\bar{2}10 \rangle$
 (c) $\{10\bar{1}1\}\langle 1\bar{2}10 \rangle$ and $\{10\bar{1}1\}\langle \bar{1}\bar{1}23 \rangle$
 (d) $\{10\bar{1}2\}\langle 1\bar{2}10 \rangle$
 (e) $\{10\bar{1}3\}\langle 1\bar{1}\bar{1}0 \rangle$
 (f) $\{11\bar{2}2\}\langle \bar{1}\bar{1}23 \rangle$
 (g) $\{11\bar{2}0\}$

Possible hcp slip systems

Table III. Independent Modes of Deformation in hcp Crystals

Direction	Plane	Crystallographic Elements	Number of Independent Mode
a	Basal Slip	(0002) $\langle 11\bar{2}0 \rangle$	2
	Prismatic Slip	$\{1\bar{1}00\}$ $\langle 11\bar{2}0 \rangle$	2
	Pyramidal Slip	$\{1\bar{1}0\}$ $\langle 11\bar{2}0 \rangle$	4
c		$\{h\bar{k}i0\}$ [0001]	
c + a	Pyramidal Slip	$\{hki\}$ * $\langle 11\bar{2}3 \rangle$	5
Twinning		$\{K_1\}$ $\langle \eta_1 \rangle$ †	0-5

* See Fig. 1.

† See Table 4.

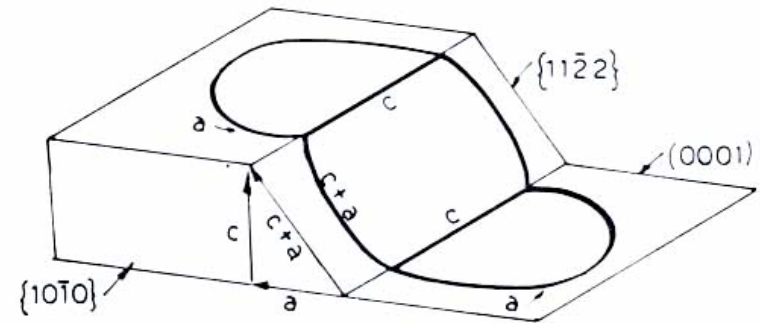
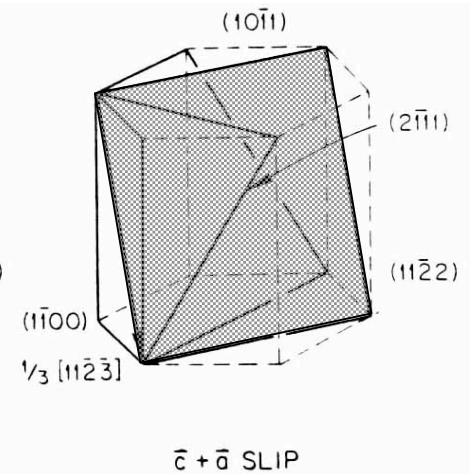
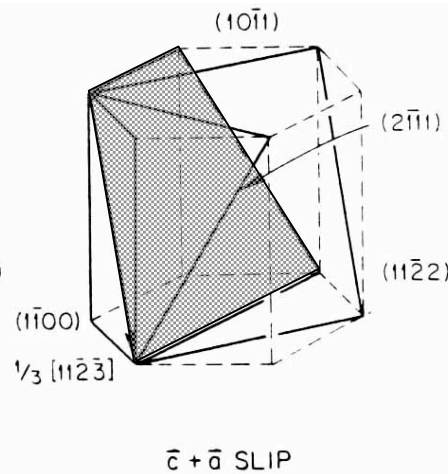
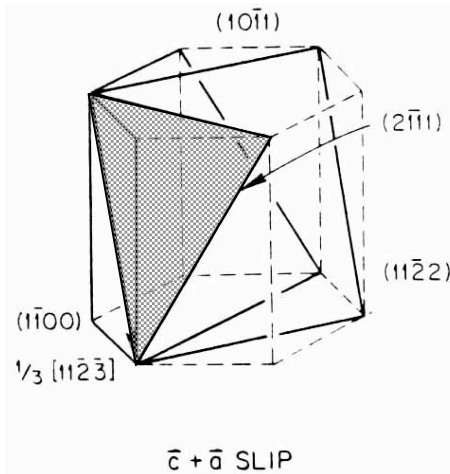
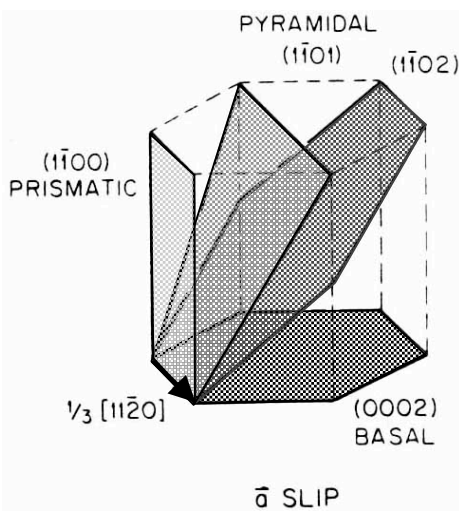


Fig. 2—c + a dislocation reaction showing decomposition of the edge component into a and c dislocations. This indicates also a source mechanism by association of a and c dislocations to form c + a screw dislocation. From Ref. 29.



Twinning as a function of Temperature

Ti crystal under compression along the c axis

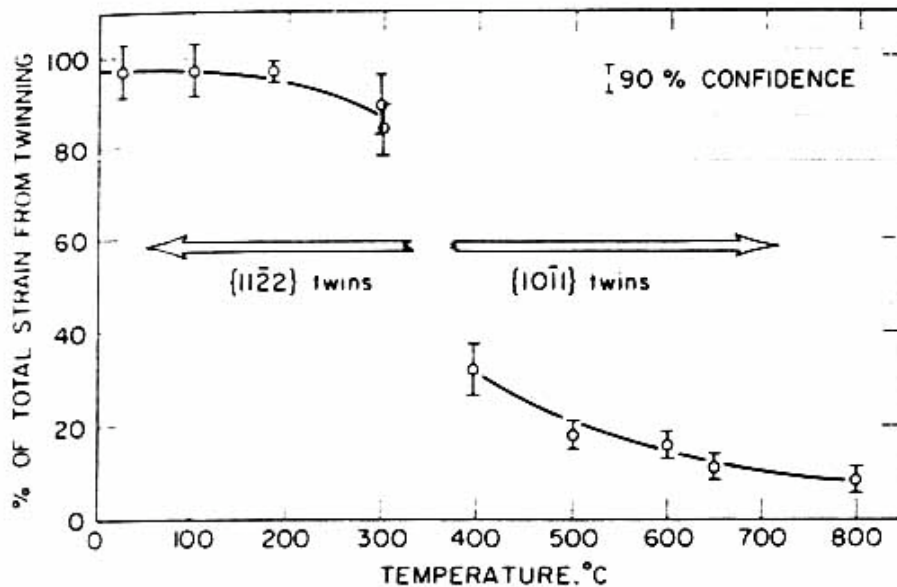
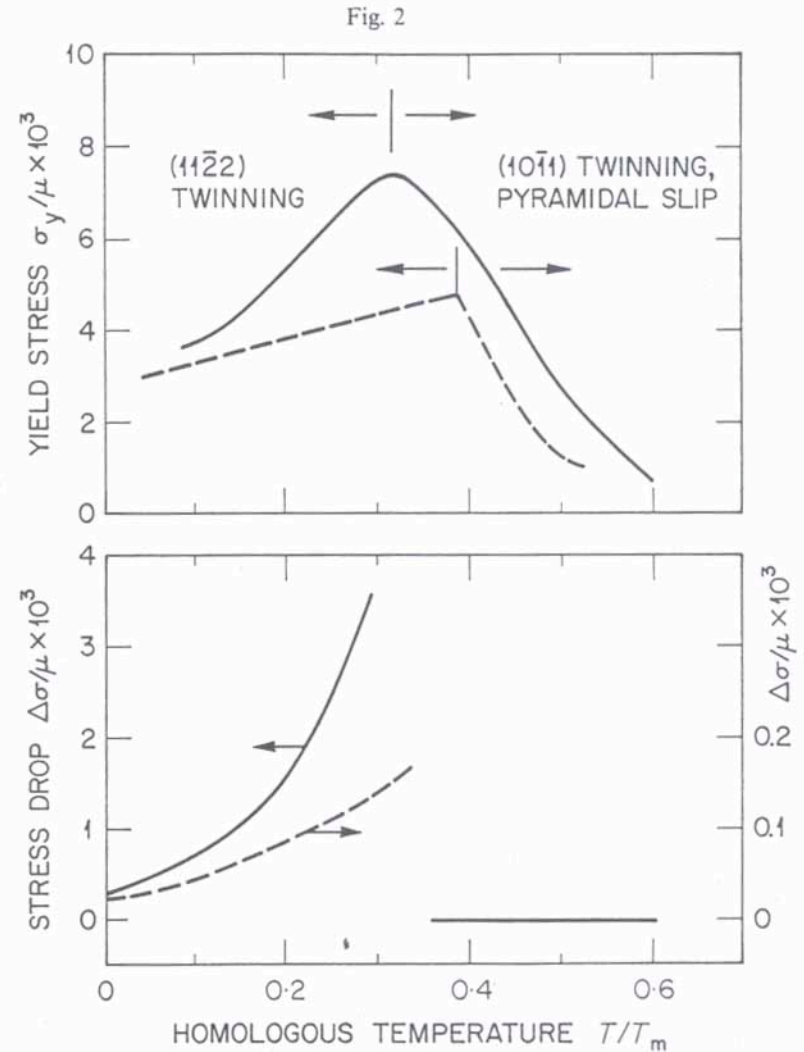


Fig. 5—The role of twinning when a Ti single crystal is compressed along the c axis. From Ref. 36.



Temperature-dependent yield strength and load drop in titanium (Paton and Backofen 1970) (—) and zirconium (Akhtar 1973) (---) under compression along the c axis.

Solid lines are Ti, dotted lines are Zr under compression along the c axis

Twinning shear vs. c/a ratio

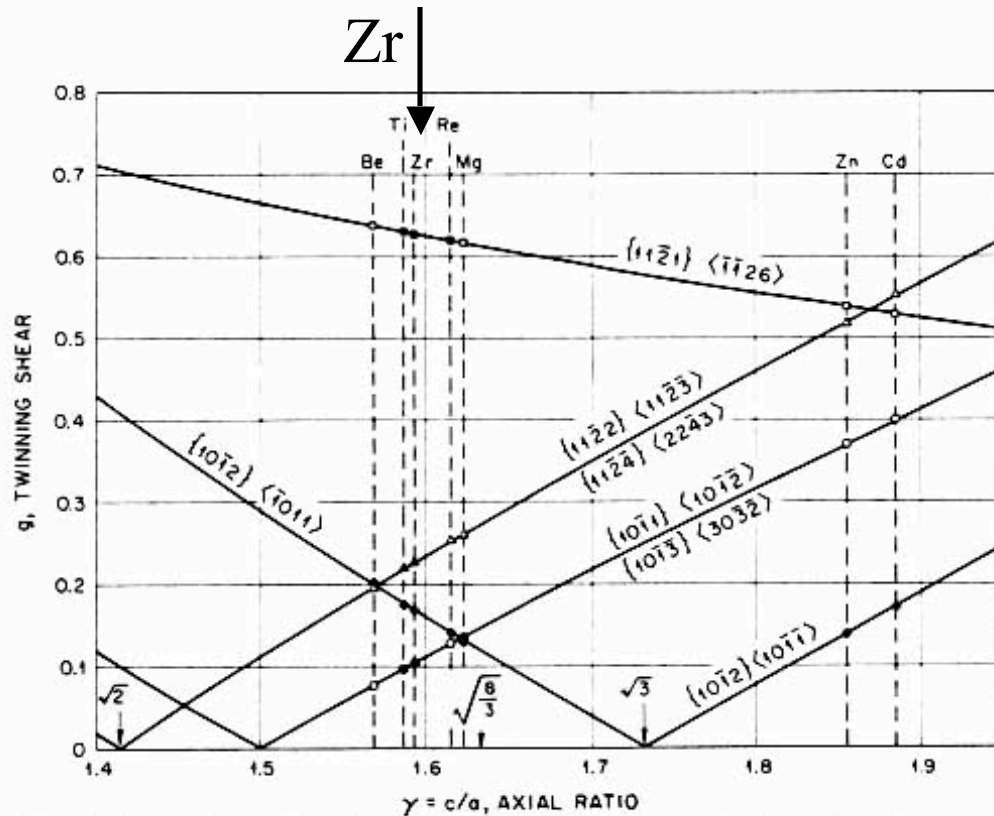


Fig. 4—Variation of twinning shear with the axial ratio. For the seven hexagonal metals, a filled symbol indicates that the twin mode is an active mode.

Twinning showing a positive slope causes a contraction along the c axis. Twinning showing a negative slope causes extension along the c axis.

Note that the $\{10\bar{1}2\}$ twin is a “compression” twin for Cd and Zn but a “tension” twin for the rest, including Ti and Zr.

K_1, K_2, η_1, η_2 notation

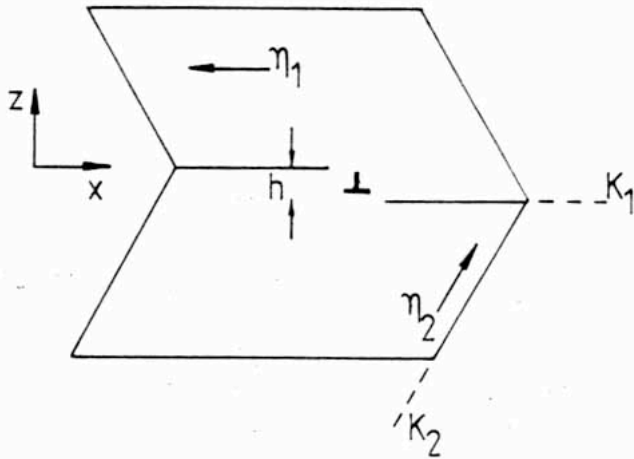


Fig. 1. Schematic illustration of a twinned crystal showing the twinning elements K_1, η_1, K_2 and η_2 , and the interfacial step associated with a twinning dislocation.

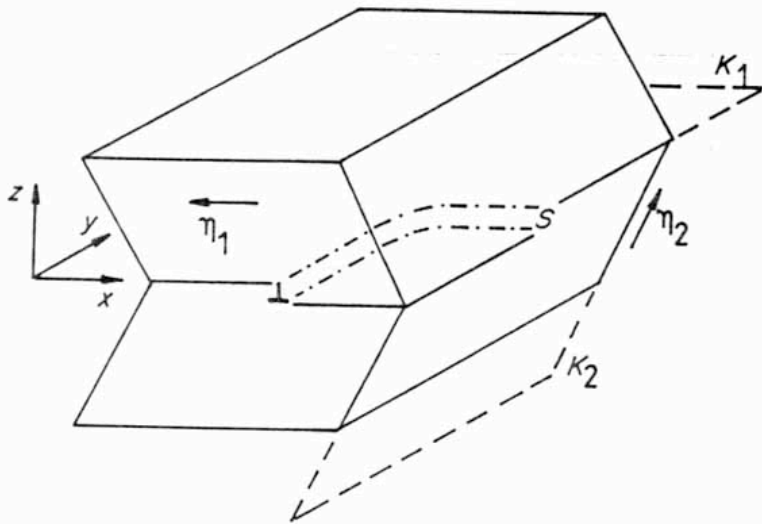


Fig. 4. Schematic illustration of a twinned crystal showing the twinning elements K_1, η_1, K_2 and η_2 , and the interfacial step associated with a twinning dislocation (of class 1 or 2).

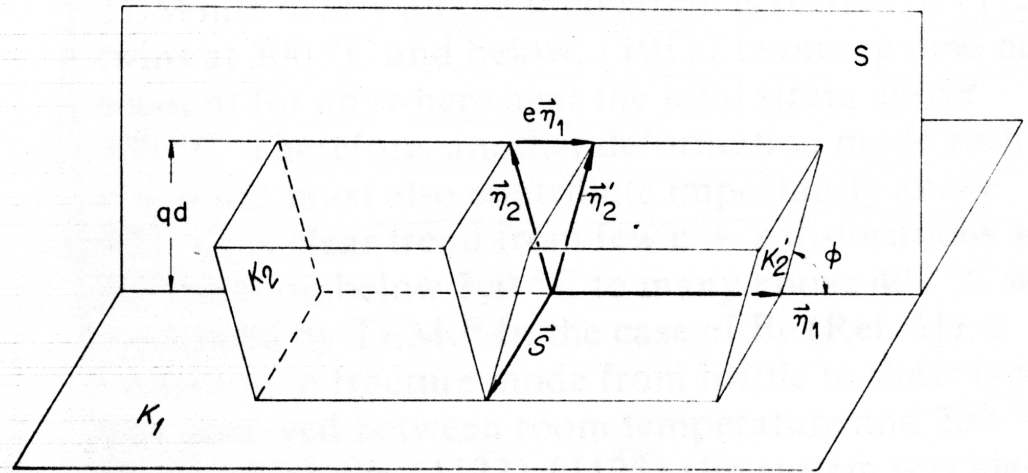


Fig. 3—Crystallographic elements of twinning. The unit cell defined by $\eta_1, \eta_2,$ and S is homogeneously sheared to the unit cell in twin defined by $\eta_1, \eta'_2,$ and S .

K_1 = twinning plane

K_2 = conjugate twinning plane

η_1 = twinning direction

η_2 = conjugate twinning direction

s = twinning shear

K_1, K_2, η_1, η_2 notation

Table IV. Crystallographic Elements and Parameters of Compound Twin Systems in hcp Structure $\gamma = c/a$

K_1	K_2	η_1	η_2	S	N_t	$\frac{N_s}{N_t}$	q	g	$e/2$	
									η_1	η_2
$\{10\bar{1}2\}$	$\{10\bar{1}\bar{2}\}$	$\pm\langle 10\bar{1}1 \rangle$	$\pm\langle 10\bar{1}\bar{1} \rangle$	$\pm\frac{1}{3} \langle \bar{1}\bar{2}10 \rangle$	8	$\frac{3}{4}$	4	$\frac{\gamma^2 - 3^*}{\gamma\sqrt{3}}$	$\frac{\gamma^2 - 3^*}{\gamma^2 + 3}$	
$\{10\bar{1}1\}$	$\{10\bar{1}\bar{3}\}$	$\langle 10\bar{1}\bar{2} \rangle$	$\langle 30\bar{3}\bar{2} \rangle$	$\frac{1}{3} \langle \bar{1}\bar{2}10 \rangle$	32	$\frac{7}{8}$	8	$\frac{4\gamma^2 - 9}{4\gamma\sqrt{3}}$	$\frac{4\gamma^2 - 9}{4\gamma^2 + 3}$	$\frac{4\gamma^2 - 9}{4\gamma^2 + 27}$
$\{11\bar{2}\bar{2}\}$	$\{11\bar{2}\bar{4}\}$	$\frac{1}{3} \langle 11\bar{2}\bar{3} \rangle$	$\frac{1}{3} \langle 22\bar{4}\bar{3} \rangle$	$\langle \bar{1}\bar{1}00 \rangle$	12	$\frac{2}{3}$	6	$\frac{2(\gamma^2 - 2)}{3\gamma}$	$\frac{\gamma^2 - 2}{\gamma^2 + 1}$	$\frac{\gamma^2 - 2}{\gamma^2 + 4}$
$\{11\bar{2}\bar{1}\}$	(0002)	$\frac{1}{3} \langle \bar{1}\bar{1}\bar{2}\bar{6} \rangle$	$\frac{1}{3} \langle 11\bar{2}0 \rangle$	$\langle \bar{1}\bar{1}00 \rangle$	8	$\frac{1}{2}$	2	$\frac{1}{\gamma}$	$\frac{1}{4\gamma^2 + 1}$	1

*Absolute value of the difference.

K_1 = twinning plane

K_2 = conjugate twinning plane

η_1 = twinning direction

η_2 = conjugate twinning direction

s = twinning shear

Notation for schematics of twins

Example: compression twin plane in Zr: $\{11\bar{2}2\}$

$\{11\bar{2}2\}$ surface

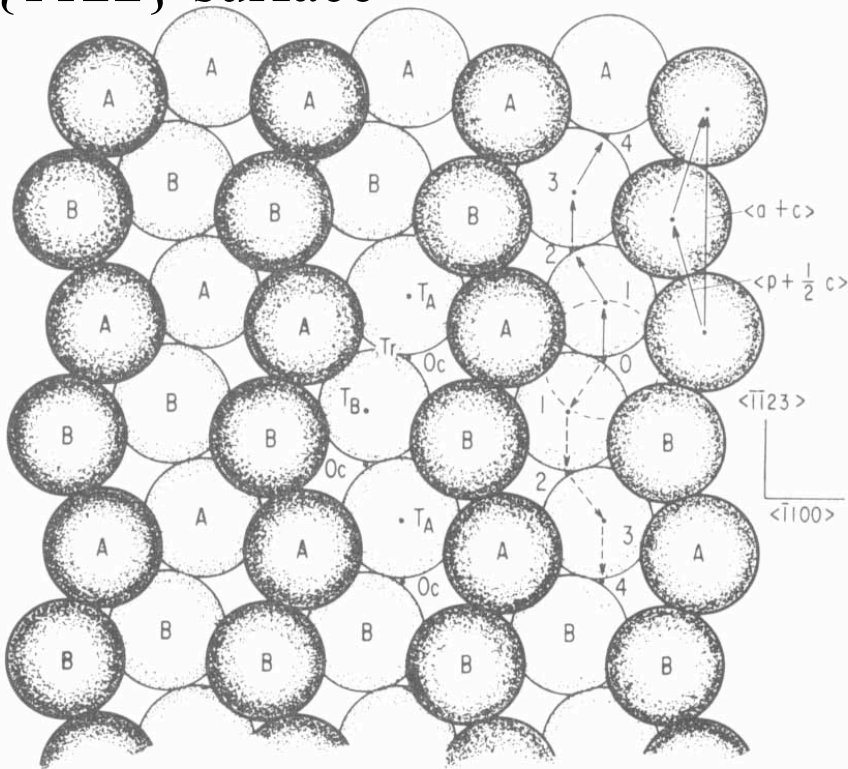
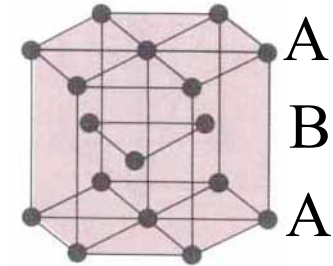
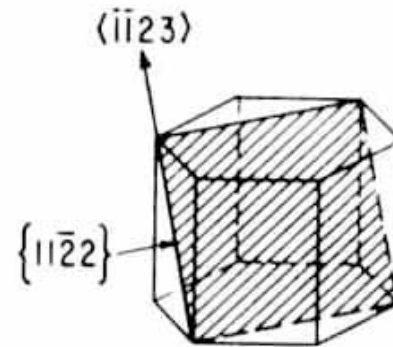
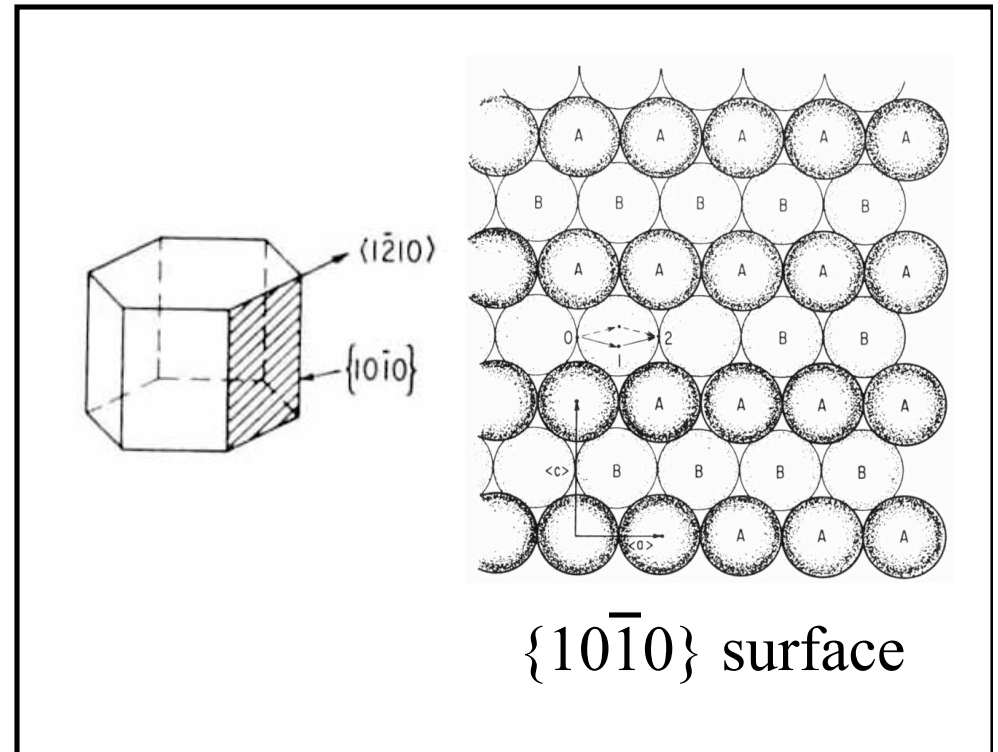


Fig. 3. A $\{11\bar{2}2\}$ surface of a hcp crystal made of closely packed spheres. Many of the spheres are labeled *A* or *B* to indicate the stacking sequence of the close-packed (0002) planes. A perfect crystal is continued by placing spheres at the octahedral positions such as those labeled *Oc*. The broken circle at 0 shows the position of one such sphere. *Tr* indicates a triangular hole. A sphere in an octahedral position simultaneously occupies a triangular position. *T_A* and *T_B* are tetrahedral positions attainable by a displacement in the $\langle\bar{1}\bar{1}23\rangle$ direction from octahedral positions on *A* and *B* planes respectively. The numbers 1, 2, 3, 4 indicate the successive positions assumed by a sphere which moves from 0 along the slip direction $\langle\bar{1}\bar{1}23\rangle$ maintaining as nearly as possible its nearest neighbor configuration. The positions 0 and 4 are octahedral positions in *A* planes while the positions 2 are in *B* planes.



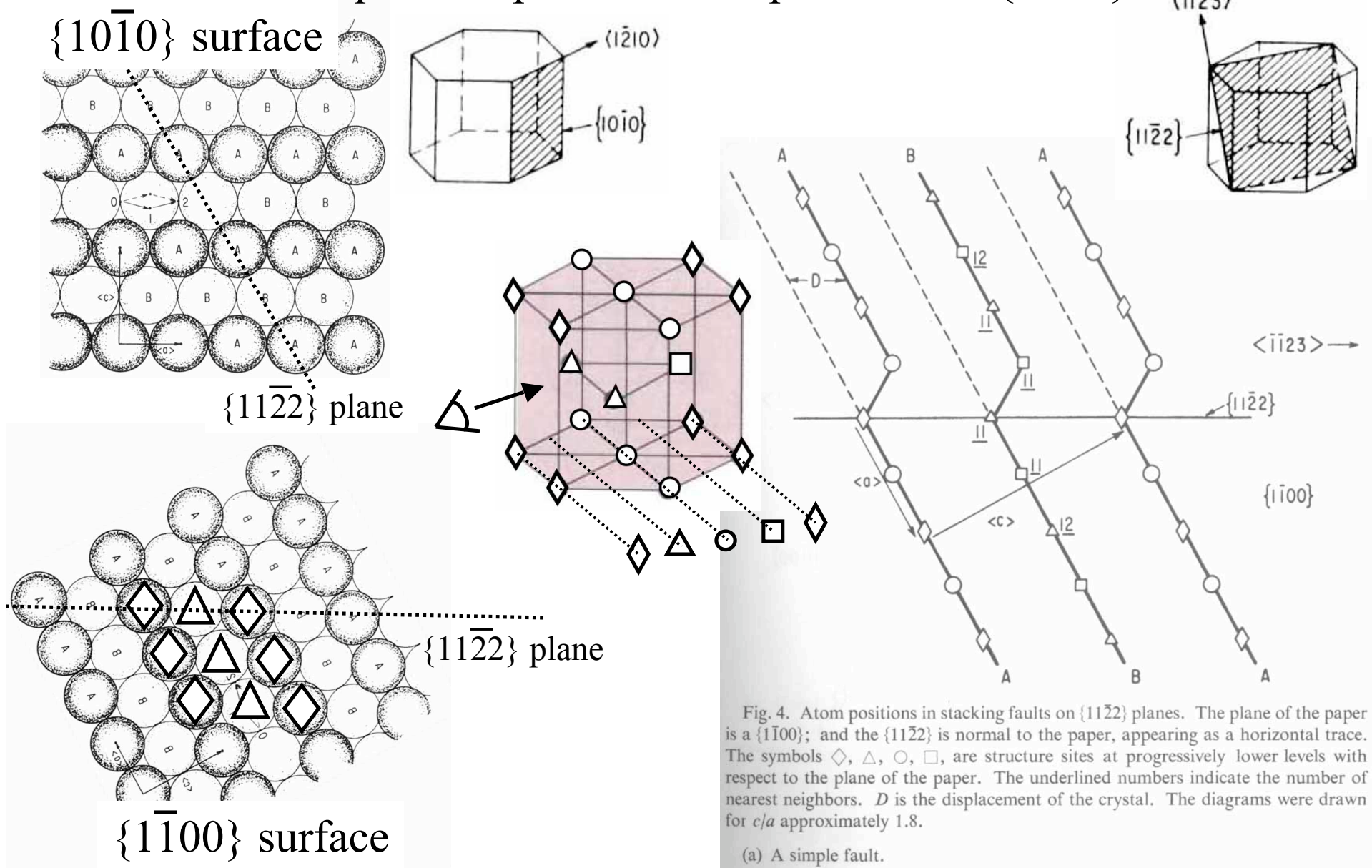
$\{11\bar{2}2\}$ surface



$\{10\bar{1}0\}$ surface

Notation for schematics of twins

Example: compression twin plane in Zr: $\{11\bar{2}2\}$



Notation for schematics of twins

Example: compression twin plane in Zr: $\{11\bar{2}2\}$

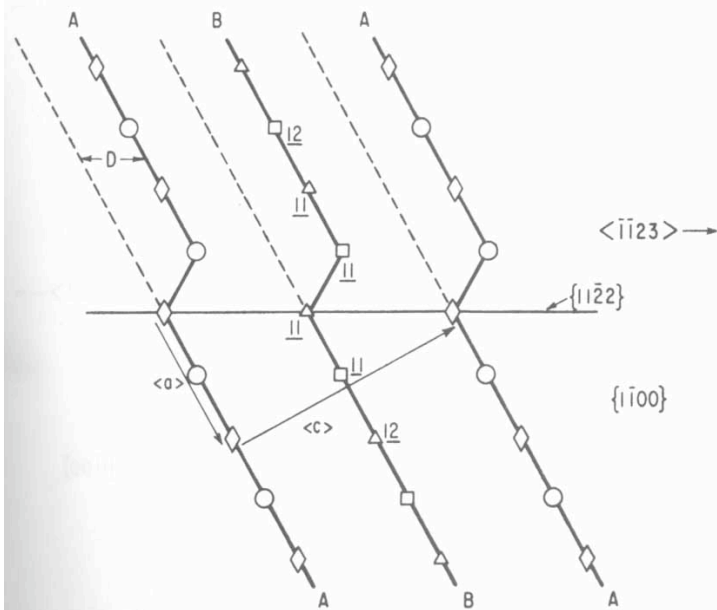


Fig. 4. Atom positions in stacking faults on $\{11\bar{2}2\}$ planes. The plane of the paper is a $\{11\bar{1}00\}$; and the $\{11\bar{2}2\}$ is normal to the paper, appearing as a horizontal trace. The symbols \diamond , \triangle , \circ , \square , are structure sites at progressively lower levels with respect to the plane of the paper. The underlined numbers indicate the number of nearest neighbors. D is the displacement of the crystal. The diagrams were drawn for c/a approximately 1.8.

(a) A simple fault.

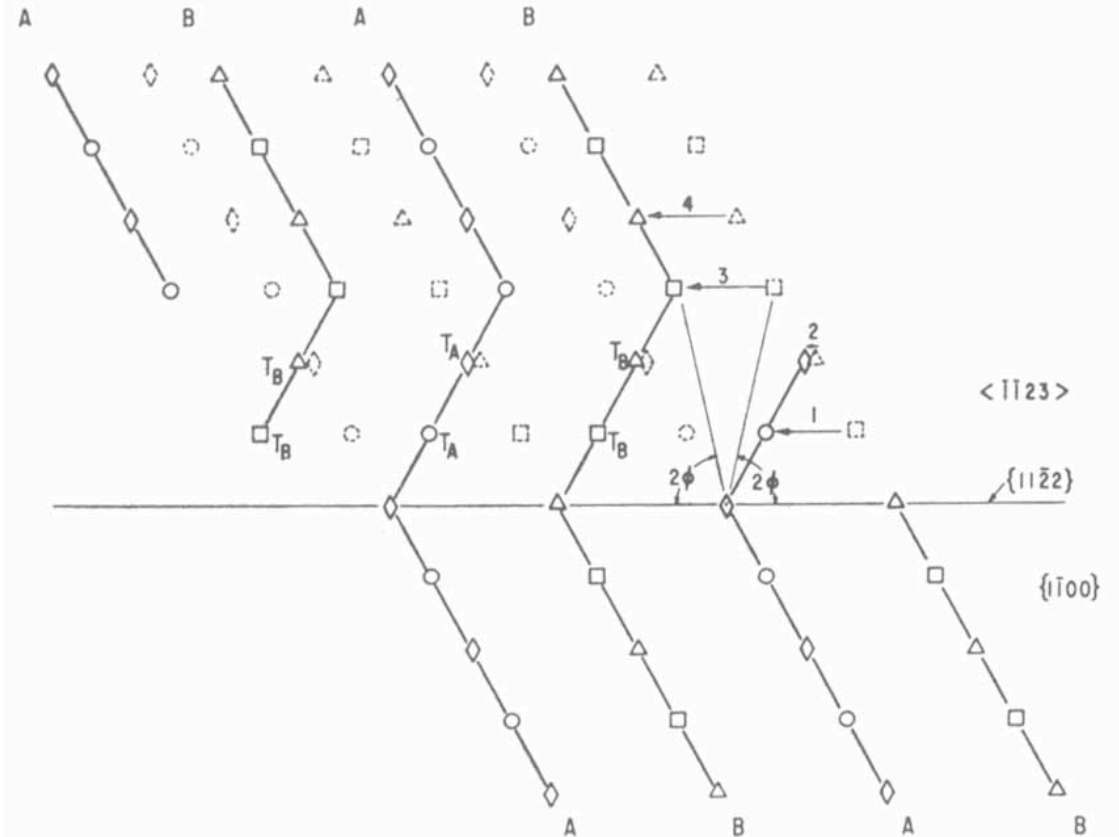


Fig. 5. Atom movements required to form a twin fault on $\{11\bar{2}2\}$ planes. Symbols are the same as in Figure 4. The angle 2ϕ defines the orientation of the second undistorted plane K_2 . In the diagram c/a is approximately 1.8. Dilatations in the twin interfaces have been ignored.

A simple fault

A twin fault on $\{11\bar{2}2\}$ plane

Dichromatic Patterns

Adjacent crystals are labeled black (μ) and white (λ), and the two lattices are projected on top of one another.

FIGURE 1. Schematic representation of the difference between a dichromatic pattern (a) and a dichromatic complex (b). (a) (001) Projection of black and white f.c.c. lattices rotated by 36.9° about [001] ($\Sigma = 5$); the space group is $I4/m\bar{m}'m'$. (b) (001) Projection of black and white lattice complexes for diamond-cubic structures having the same relative orientation as in (a); the space group is $I4\bar{2}'m'$. Large and small circles represent sites at levels 0 (or 1) and $\frac{1}{2}$ along [001] respectively; large and small squares represent sites at levels $\frac{1}{4}$ and $\frac{3}{4}$ respectively. Two-coloured symbols are neutral (grey) sites. (This diagram is also the projection for sphalerite-type structures: see text.)

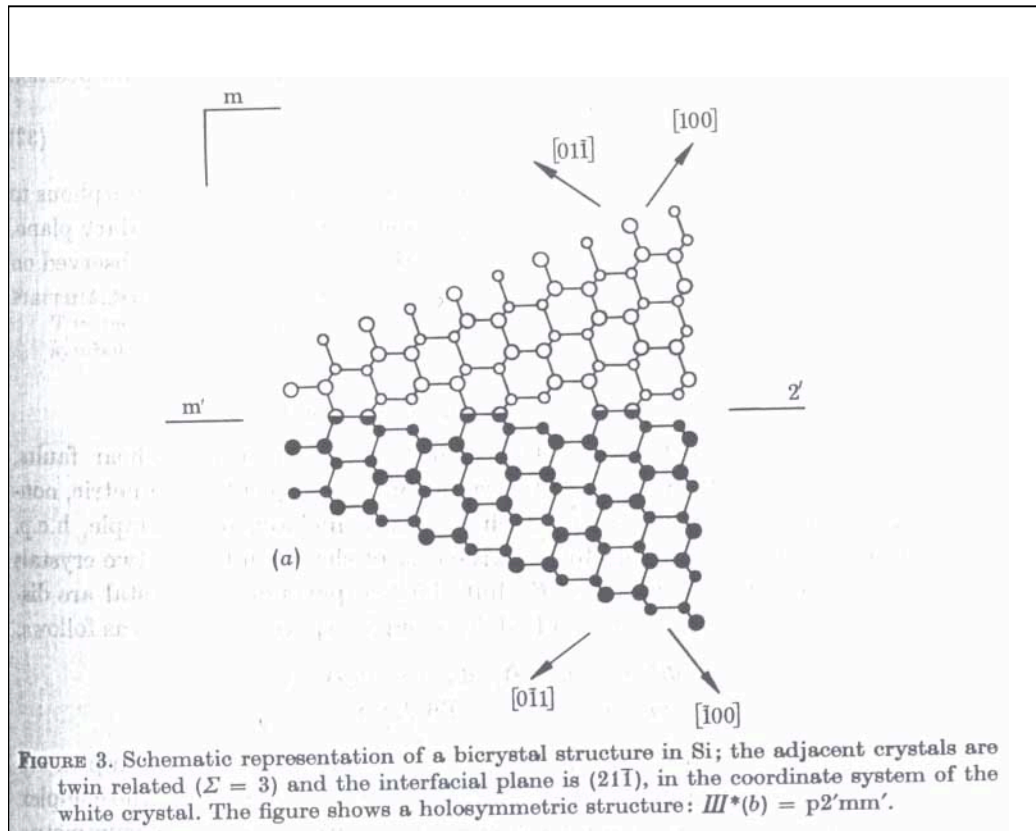
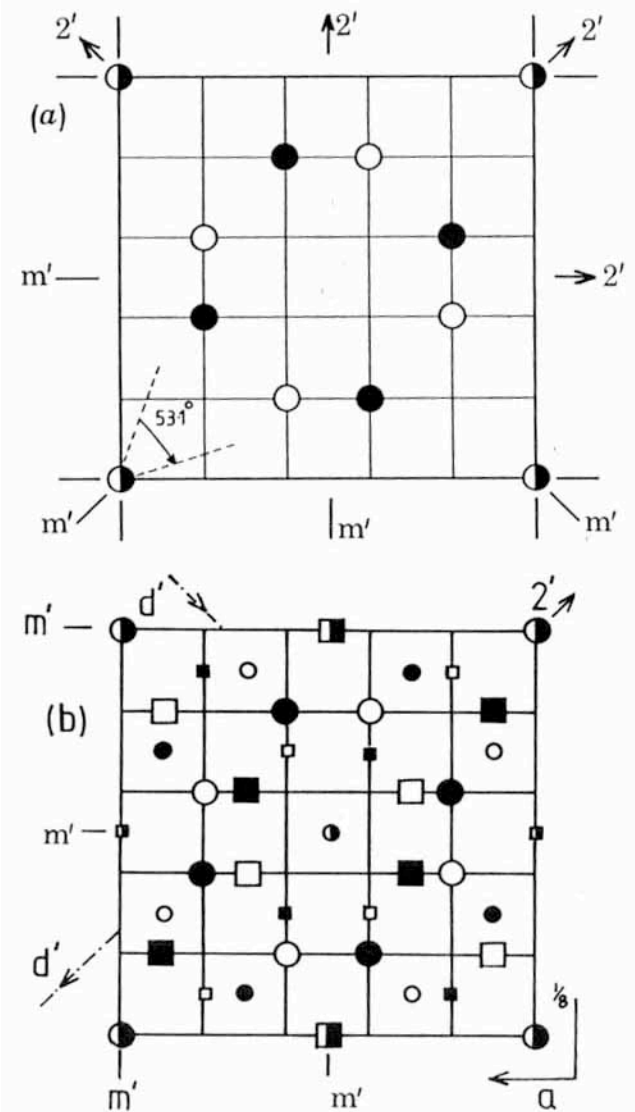


FIGURE 3. Schematic representation of a bicrystal structure in Si; the adjacent crystals are twin related ($\Sigma = 3$) and the interfacial plane is $(21\bar{1})$, in the coordinate system of the white crystal. The figure shows a holosymmetric structure: $III^*(b) = p2'mm'$.

Burgers Vectors Notation

Bicrystal is imagined to be created by joining white (λ) and black (μ) crystals (fig a). Interface dislocations arise when the black and white crystal surfaces have surface features which are not complimentary (fig b & c).

In figure b, the steps are characterized by the translation vectors $t(\lambda)_j$ and $t(\mu)_i$. By joining the two crystal surfaces so the interfacial structures are identical on either side of the perturbations, a dislocation is introduced with the Burgers vector of:

$$\mathbf{b}_{ij} = \mathbf{t}(\lambda)_j - \mathbf{P}\mathbf{t}(\mu)_i$$

when written in the λ frame, where \mathbf{P} expresses the relationship between the co-ordinate frames of the two crystals.

Note: the vector \mathbf{n} is perpendicular to the μ surface

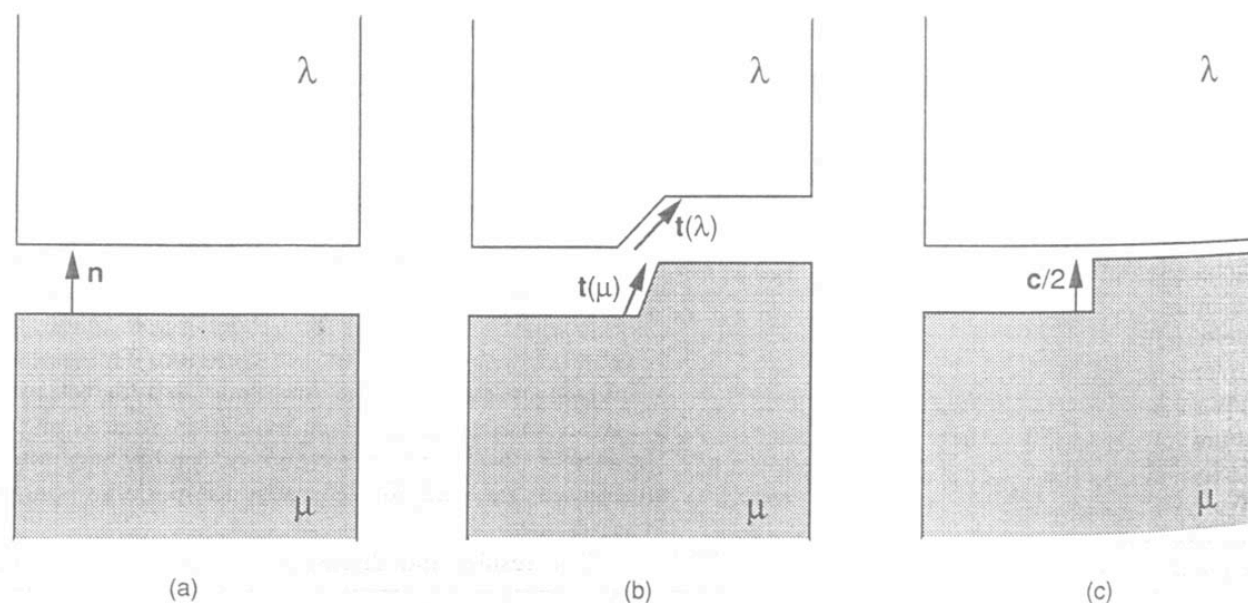


Fig. 1. (a) Schematic illustration of the formation of a bicrystal by joining white (λ) and black (μ) half-crystals. (b) Formation of an interfacial defect by joining crystal surfaces with incompatible steps. (c) Formation of a defect by joining demisteppped and unstepped surfaces.

Burgers Vectors Notation

The magnitude of the normal component of \mathbf{b}_{ij} is designated b_z and is equal to the difference between the two surface step heights (h) expressed in the λ frame.

$$h(\lambda)_j = \mathbf{n} \cdot \mathbf{t}(\lambda)_j$$

$$h(\mu)_i = \mathbf{n} \cdot \mathbf{P}\mathbf{t}(\mu)_i$$

$$b_z = h(\lambda)_j - h(\mu)_i$$

It is convenient to designate the total Burgers vector by an appropriate subscript. For twins, Burgers vectors are written as

$b_{p/q}$ where p and q are defined as:

$$h(\lambda)_j = pd \quad \text{and} \quad h(\mu)_i = qd$$

Where d is the interplanar spacing, i.e. $d_{(10\bar{1}2)}$ for the $(10\bar{1}2)$ lattice planes.

Owing to symmetry: $b_{p/q} = -b_{-p/-q}$ and for the pairs $b_{p/q}$ and $b_{q/p}$ the components b_x and b_y are the same but the b_z components are opposite.

Burgers Vector Notation

$[1\bar{2}10]$ projection of the dichromatic pattern associated with the $(10\bar{1}2)$ twin boundary.

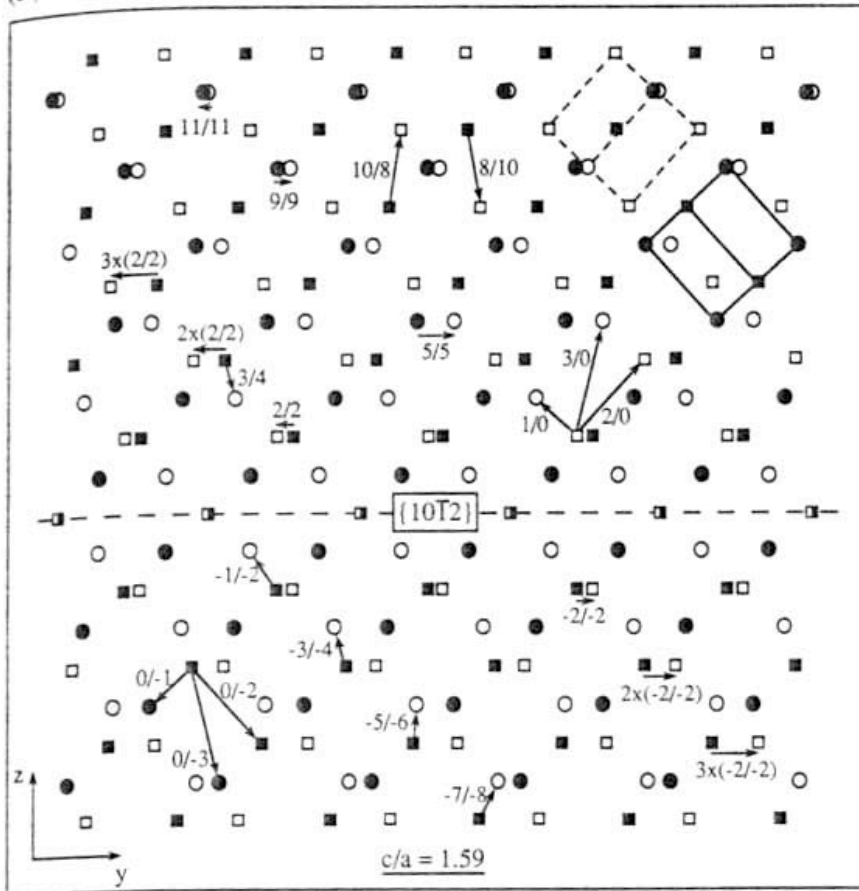
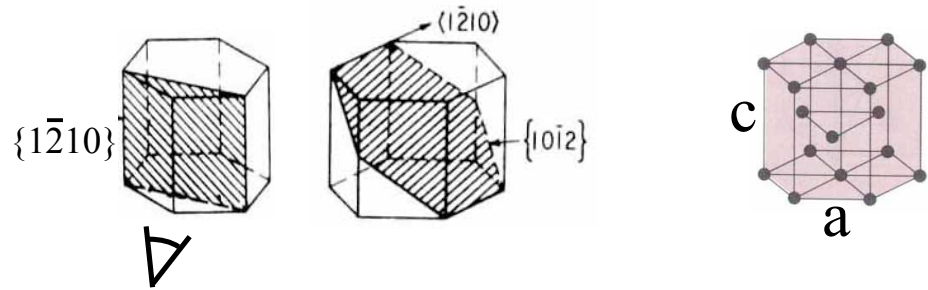


Fig. 2. $[1\bar{2}10]$ projection of the dichromatic pattern associated with (a) the $(10\bar{1}2)$ twin boundary and (b) the incommensurate 90° -tilt boundary in Ti. The outline of hexagonal unit cells in the λ and μ crystals are indicated, as are the p/q values used to define the Burgers vector of the selected crystal and interfacial dislocations, as explained in Section 2.



The Burgers vectors for crystal dislocations, for which h is always zero, can be represented in this notation. For example, defects in the λ crystal with:

$\mathbf{b} = \mathbf{a}$ are either $b_{1/0}$ or $b_{0/0}$

$\mathbf{b} = \mathbf{c}$ are $b_{2/0}$

$\mathbf{b} = \mathbf{c} + \mathbf{a}$ are $b_{3/0}$

The screw component of \mathbf{b} is not represented explicitly in this notation. For example: the screw dislocation with $\mathbf{b}=\mathbf{a}$, parallel to the interface, can be defined as $b_{0/0} = 1/3[1\bar{2}10]$

Dichromatic pattern of the twin

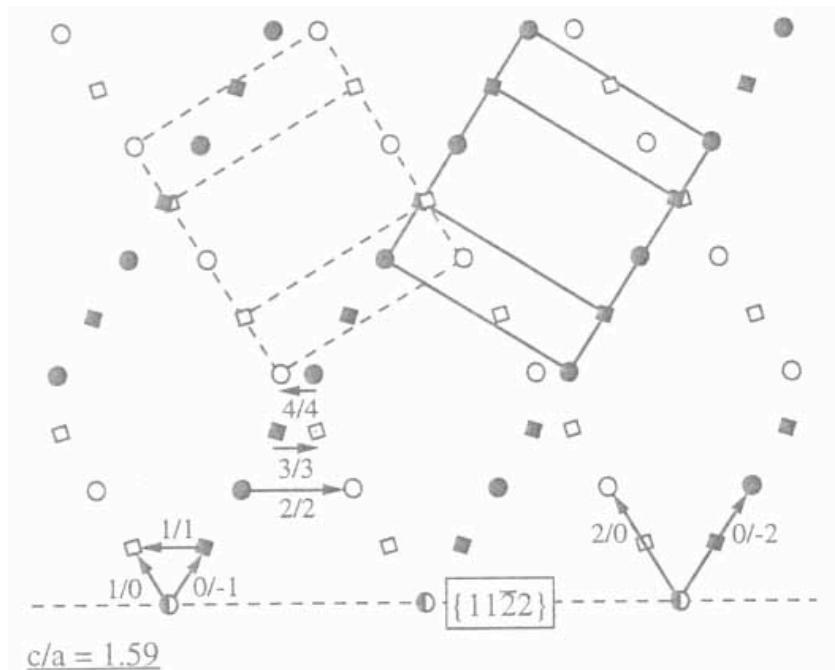
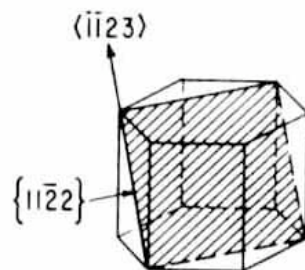
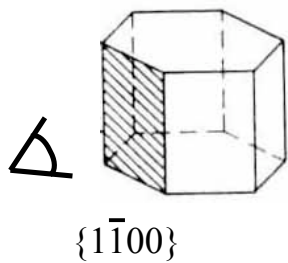


Fig. 1— $\langle 1\bar{1}00 \rangle$ projection of the dichromatic pattern for the $\{11\bar{2}2\}$ twin boundary showing Burgers vectors on arrows. The outline of a hexagonal unit cell is superimposed on each crystal and the circle and square symbols indicate the stacking of the $\{1\bar{1}00\}$ lattice planes.

$\langle 1\bar{1}00 \rangle$ projection of the $\{11\bar{2}2\}$ twin, with the set of burgers vectors of admissible interface dislocations indicated by arrows

$b_{1/1}$ indicates interface step of one interplanar distance

$b_{3/3}$ indicates interface step of three interplanar distances



$b_{3/3}$ has narrow core and is sessile in computer model, while $b_{1/1}$ has wide core and high mobility.

However, the sense of twinning shear is the reverse of that found in practice.

Schematics of hcp twins

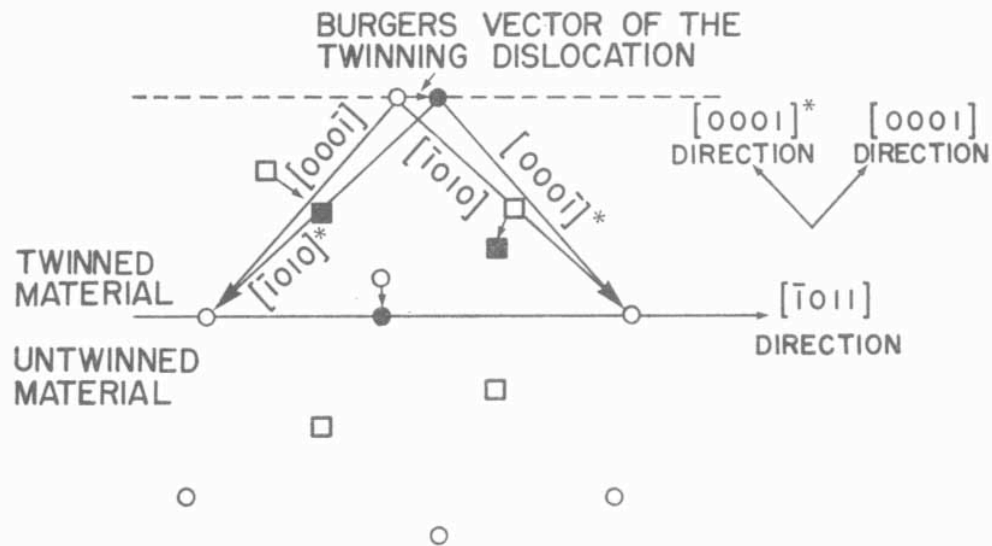


Fig. 4. Twinning on $(10\bar{1}2)$ planes in zirconium. Projection of the lattice on the $(\bar{1}2\bar{1}0)$ plane. Circles are in the plane of the page. Squares are $a/2$ above and below the page. Solid symbols indicate atom positions in the twin. (After reference 14.)

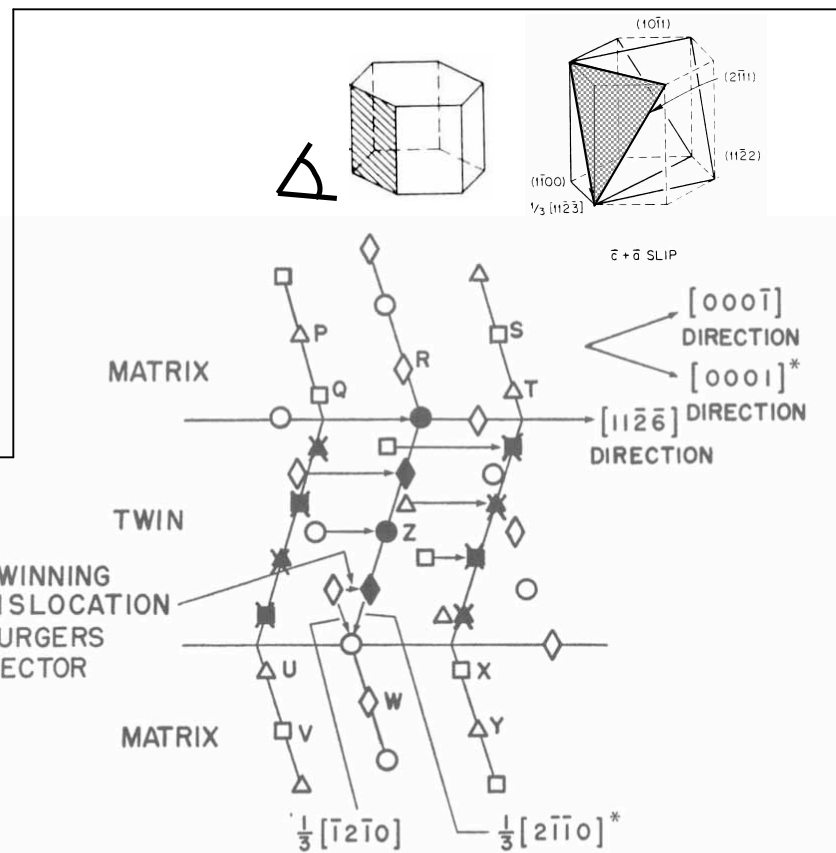
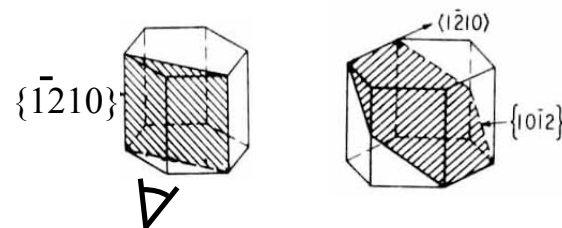


Fig. 9. Projection of the zirconium lattice on the (1100) plane. Solid symbols represent atom positions in the twin. Circles are in the plane of the page. Squares are $\sqrt{3}a/3$ below the page, diamonds are $\sqrt{3}a/2$ below the page, and triangles are $5\sqrt{3}a/6$ below the page. An X superimposed on a symbol indicates that it is shifted $\sqrt{3}a/6$ closer to the page.

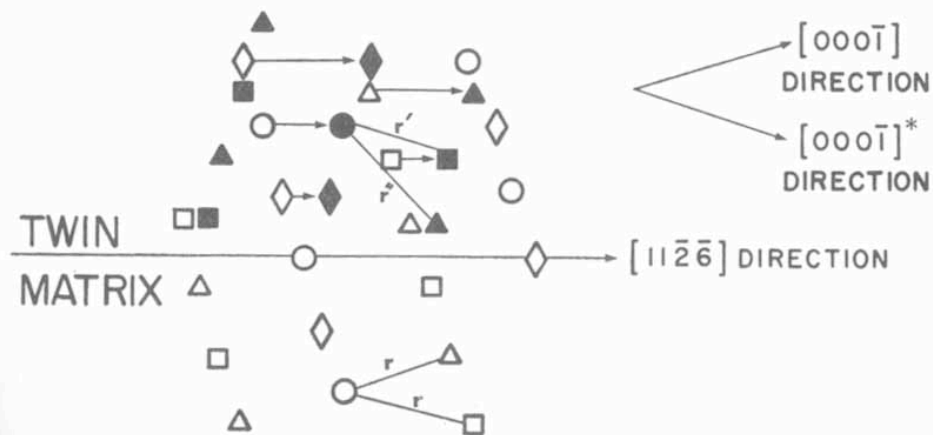
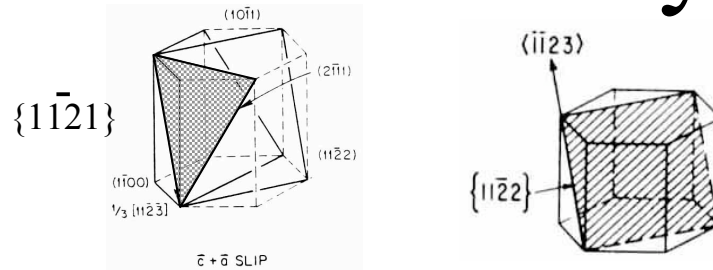


Fig. 7. Zirconium lattice projected on the $(1\bar{1}00)$ plane. Solid symbols show atom positions after homogeneous shear on $(11\bar{2}1)$ planes. Circles are in the plane of the page. Squares, diamonds and triangles are in first, second and third planes below the page.

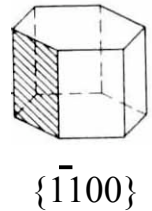
The model used by Serra, Bacon, and Pond

- Simulations were carried out by a many-body interatomic potential of Finnis-Sinclair type for α -titanium, as derived by Ackland, *et.al.*
- Crystal models of this type exhibit proper:
 - c/a lattice parameter ratio,
 - Elastic constants,
 - Stacking fault energies
- They do NOT describe:
 - The directional nature of bonding inherent in transition metals
 - The potential favors basal slip, while prism slip is preferred in the real metal.
- The simulations are best considered as those of a model hcp system.

The model used by Serra, *et.al.*



- Perfect $(11\bar{2}1)$ and $(11\bar{2}2)$ twins were created in the relaxed state with periodic boundary conditions along the $[1\bar{1}00]$ axis
 - Inner relaxable region contained up to 3000 atoms
 - Thickness along $[1\bar{1}00]$ equal to the repeat distance of the lattice, $\sqrt{3}a$
 - The dislocation was parallel to the interface due to the periodicity requirements.



Approach & Results of Serra, *et.al.*

- Applied a shear stress resolved for basal slip to a $\{10\bar{1}2\}$ twinned bicrystal
 - Screw dislocations with $b=1/3\langle 11\bar{2}0\rangle$ and line direction parallel to the boundary (also called $b_{0/0}$) are able to cross the twin interface
 - No residual dislocations are left behind.
 - Cross-slip is facilitated by core constriction at the boundary, but interface is still a significant barrier to glide.

Approach & Results of Serra, *et.al.*

- Similar modeling of $\{10\bar{1}1\}$ twins revealed:
 - Total absorption of the screw dislocation by its transformation into a pair of twinning dislocations.
- Computer modeling of $\{10\bar{1}2\}$ twin boundary and a perfect dislocation gliding on the (0001) plane with b inclined at 60 deg to the dislocation line (also called $b_{1/0}$):
 - Slip was not transferred from one crystal to the other, instead the dislocation decomposes into boundary dislocations, also referred to as interfacial defects.

$$b_{1/0} = b_{-5/-6} + 3b_{2/2}$$

- This results in a source for new twinning dislocations, which produces further twinning growth.

A. Serra, R.C. Pond, D.J. Bacon, "Computer Simulation of the Structure and Mobility of Twinning Dislocations in HCP Metals," Acta Metall.Mater. vol 39, 1991, p 1469.

A. Serra, D.J. Bacon, R.C. Pond, "Twins as barriers to basal slip in hexagonal-closed-packed metals," Metallurgical and Materials Transactions A, vol 33A, March 2002, p 809.

Results of Serra, et.al.

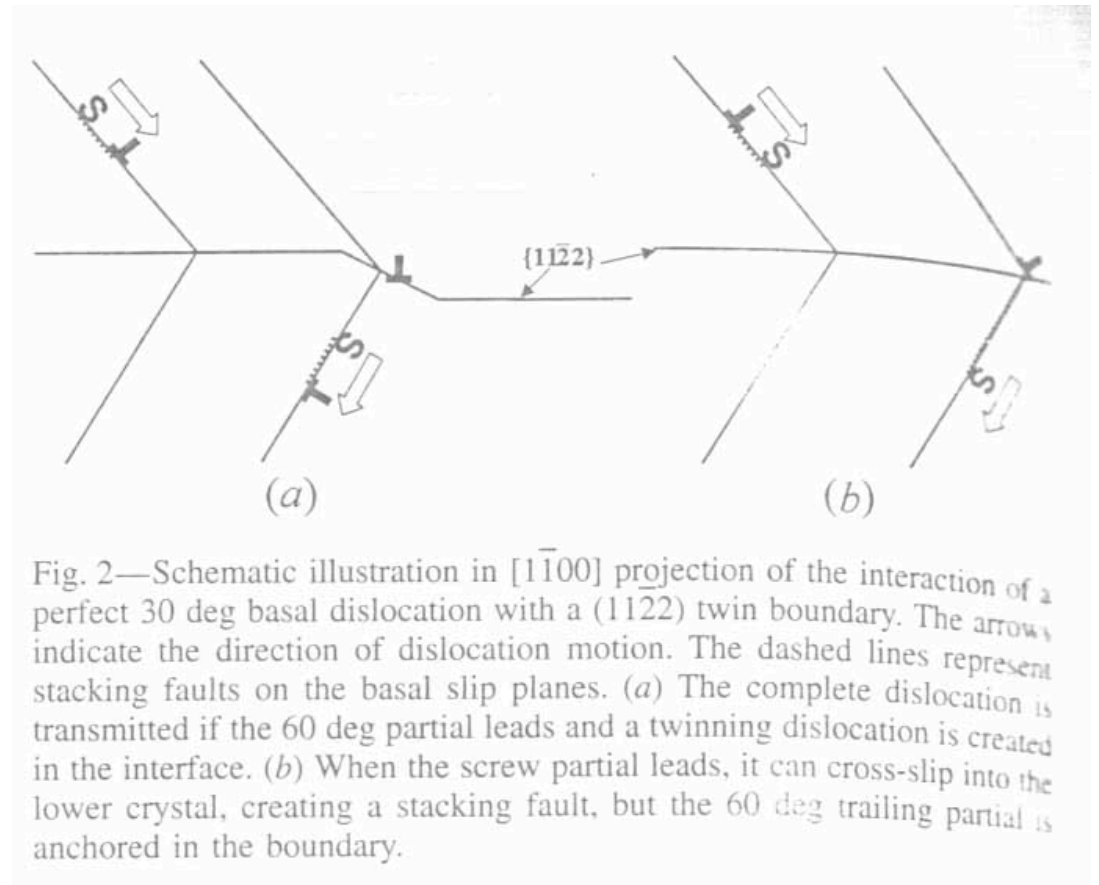
- $\{1\bar{1}22\}$ twin boundary, with 30 deg dislocation, $b_{1/0}$
 - Dislocation dissociates into two shockley partials in the perfect crystal, i.e. a screw partial and a 60 deg partial.
 - When the dislocation interacts with the 60 deg partial leading it is stopped by the boundary
 - With increased applied shear stress the following reaction occurs:

$$b_{-1/0} = b_{-1/-1} + b_{0/1}$$

- This creates a twinning dislocation that allows the crystal dislocation to cross the boundary and continue to glide in the next crystal. (See fig 2a)

Results of Serra, et.al.

- When the screw partial leads, it can cross slip into the next crystal without resistance, leaving the 60 deg partial at the interface.
- Since the previously noted reaction is not possible, this leaves the partial anchored at the boundary. (see figure 2b)



Results of Serra, et.al.

- $\{1\bar{1}22\}$ twin boundary, with edge dislocation $b_{-2/0}$
 - Dislocation dissociates into two 60 deg partials in the basal plane in the model crystal.
 - Reaction:
$$b_{-2/0} = 2b_{-1/-1} + b_{0/2}$$
 - The first dislocation can decompose into two twinning dislocations and a perfect edge dislocation in the other crystal.

Results of Serra, et.al.

- The $\{11\bar{2}1\}$ twin is similar to the $\{11\bar{2}2\}$ twin, and the previous two reactions can occur in principle.
- Due to symmetry of the bicrystal, another reaction is possible: $b_{1/2/1/2}$
- This dislocation is very wide and has much lower energy, and is very mobile.

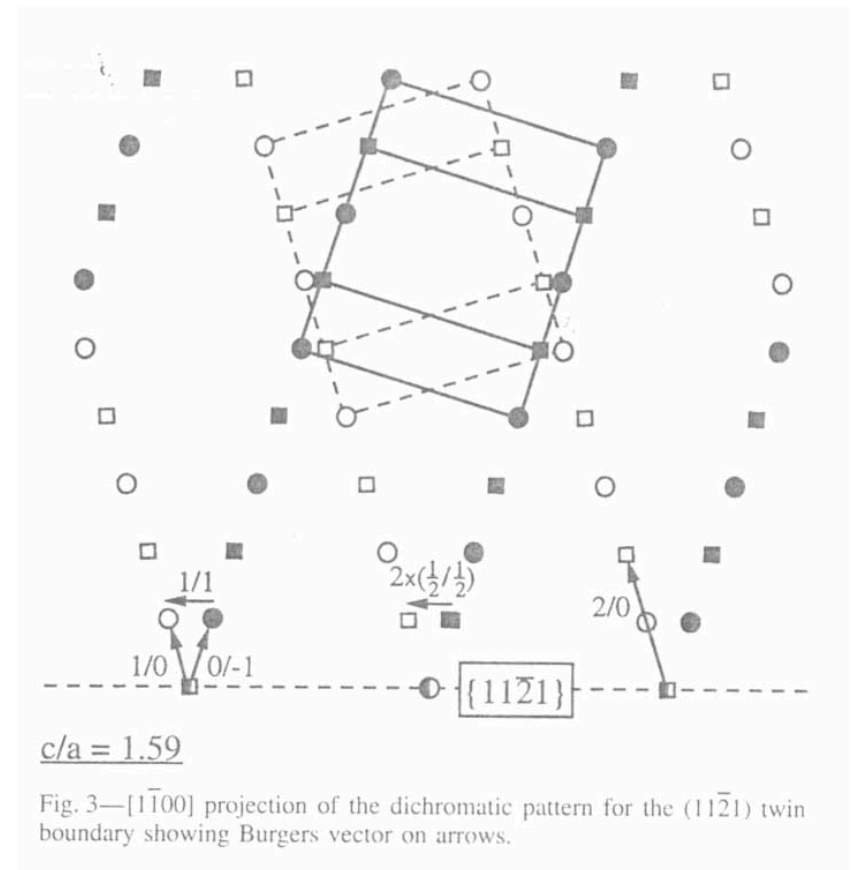
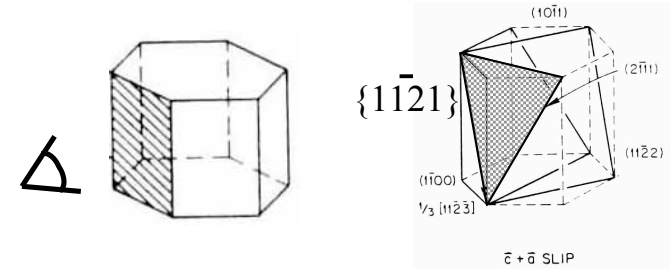


Fig. 3— $[11\bar{0}0]$ projection of the dichromatic pattern for the $(11\bar{2}1)$ twin boundary showing Burgers vector on arrows.

Results of Serra, et.al.

- The $\{11\bar{2}1\}$ twin interaction with the 30 deg dislocation $b_{1/0}$:
 - When the 60 deg partial leads, the complete dislocation is transmitted through the boundary
 - If the screw partial leads, it is still transmitted, although the stress required is much higher.
- The $\{11\bar{2}1\}$ twin interaction with the 30 deg dislocation $b_{-2/0}$:
 - This dislocation is stopped by the boundary and is not even partially transmitted to the other crystal.
 - The change in the stacking sequence of the basal plans when crossing the twin boundary is a strong barrier.

Conclusions

- Serra, Bacon, and Pond have done many computer simulations of hcp twins and dislocation/twin interactions, only a few of which I have shown here.
- The reactions discussed in this talk included:
 - $\{10\bar{1}2\}$ twin and $b_{0/0}$ and $b_{1/0}$
 - $\{10\bar{1}1\}$ twin and $b_{0/0}$
 - $\{11\bar{2}2\}$ twin and $b_{1/0}$ and $b_{-2/0}$
 - $\{11\bar{2}1\}$ twin and $b_{-2/0}$ and $b_{1/0}$ and $b_{1/2/1/2}$